Student thesis series INES nr 396

Analysis of Arctic peak-season carbon flux estimations based on four MODIS vegetation products

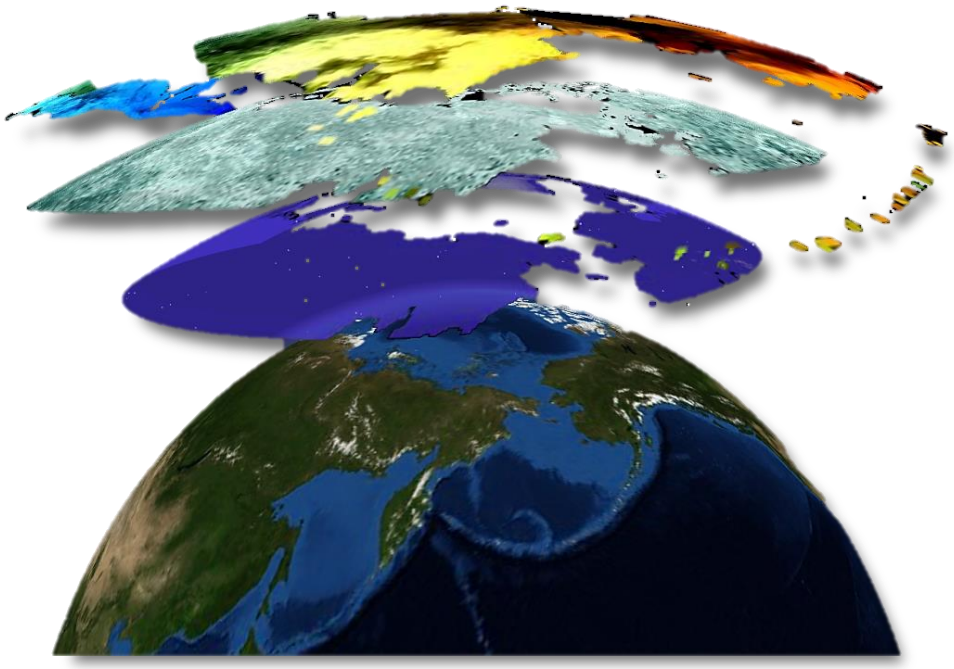

Antonín Kusbach

2016
Department of
Physical Geography and Ecosystem Science
Lund University
Sölvegatan 12
S-223 62 Lund
Sweden

Antonín Kusbach (2016)

Analysis of Arctic peak-season carbon flux estimations based on four MODIS vegetation products

Analys av kolflöde under arktis högsäsong uppskattning baserad på fyra MODIS produkt vegetation

Master degree thesis, 30 credits in *Master Degree Project*
Department of Physical Geography and Ecosystem Science, Lund University

Level: Master of Science (MSc)

Course duration: *November* 2015 until *June* 2016

Cite as:

Kusbach, A., 2016. Analysis of Arctic peak-season carbon flux estimations based on four MODIS vegetation products. MSc thesis. Lund University, Department of Physical Geography and Ecosystem Science, Sweden.

Disclaimer

Analysis of Arctic peak-season carbon flux estimations based on four MODIS vegetation products

---

Antonín Kusbach

Master thesis, 30 credits, in *Physical Geography and Ecosystem Analysis*

(*nge14aku@student.lu.se*)

Dr. Andreas Persson

Project supervisor

Department of Physical Geography and Ecosystem Science

Dr. John Connolly

Co-supervisor

School of History & Geography, DCU St. Patrick's Campus, Dublin, Ireland

Exam committee:

Maj-Lena Linderson, Department of Physical Geography and Ecosystem Science

Jörgen Olofsson, Department of Physical Geography and Ecosystem Science

Antonin Kusbach

Analysis of Arctic peak-season carbon flux estimations based on four MODIS vegetation products

Abstract (English)**.** Increased temperatures in high latitudes may alter the carbon dynamics throughout the Arctic. Modelled CO_2 simulations show that current climate conditions constitute the Arctic a net carbon sink, though the large extent and fine landscape heterogeneity raise an uncertainty about the carbon sink/source status of the region. The understanding of Arctic CO_2 fluxes can be improved through integration of remote sensing techniques and environmental modelling. In this study, vegetation indices, i.e. LAI and NDVI from four MODIS products are used in the Pan-Arctic Net Ecosystem Exchange (PANEEx) model to calculate NEE at 12 Arctic study sites. The main objective was to determine the impact of the vegetation indices at 250 m, 500 m and 1 km resolution on the precision of NEE estimations. Data from eddy covariance towers (EC) were used to identify similarities and discrepancies between modelled and *in situ* LAI and NEE scores in July 2008-2010. Google Earth Engine (Google Inc.), a powerful geospatial platform, was implemented for data acquisition and quantitative analysis. Linear correlations on 1:1 scatter plots and inferential statistics were used to assess the relationships between the modelled and *in situ* estimations. The model run using the 250 m MOD13Q1 LAI product simulated 78% of the measured NEE fluxes ($R^2 = 0.73$, $p < 0.001$) throughout the study sites. Overall, utilization of the PANEEx model with 250 m MODIS products indicates a potential for future modelling in the Arctic. Data analysis generated considerable differences in modelled NEE outputs and hence, their application in environmental modelling needs to be considered. The model simulations also demonstrate the potential of employing vegetation indices on much finer scale, i.e. 10-30 m in order to capture the Arctic heterogeneous landscape.

Key words: Arctic, net ecosystem exchange, vegetation indices, satellite-derived data, big data analysis

List of abbreviations:

CO_2- Carbon dioxide

EC – Eddy covariance

GEE – Google Earth Engine

GPP- Gross primary production

LAI – Leaf area index

LRC – Light response curve

MODIS – Moderate Resolution Imaging Spectroradiometer

NDVI – normalized difference vegetation index

NEE- Net ecosystem exchange [µmol m^{-2} s^{-1}]

PANEEx – Pan-Arctic net ecosystem

Antonin Kusbach

Analys av kolflöde under Arktis högsäsong uppskattning baserad på fyra MODIS produkt vegetation

Sammanfattning (Svenska). Förhöjda temperaturer på höga breddgrader kan förändra koldynamiken i hela Arktis. Modellerade CO_2 simuleringar visar att under nuvarande klimatförhållanden utgör Arktis en netto kolsänka, fast den stora utsträckningen samt fina geografiska heterogenitet lyfter upp osäkerhet kring dess status som CO_2 sänka/källa i regionen. Förståelsen för arktiska koldioxidflödekan förbättras genom integrering av fjärranalys och miljömodellering. I denna studie används fyra MODIS vegetations index (NDVI & LAI) som används i en simpel Pan-Arctic Net Ecosystem Exchange (PANEEx) modell för att beräkna NEE vid 12 arktiska undersökningsområden. Huvudsyftet var att bedöma effekten av fyra olika vegetationer index på precisionen av NEE uppskattningar de fyra indexen har upplösningarna 250 m, 500 m och 1 km. Data från eddy covariance torn (EC) användes för att identifiera likheter och skillnader mellan modellerade och platsbaserade LAI och NEE mätningar mellan juli 2008 till 2010. Google Earth Engine (Google Inc.), en kraftfull geospatial plattform, användes för datainsamling och kvantitativ analys. Linjära korrelationer på 1:1 spridningsdiagram och trendanalys användes för att bedöma förhållandet mellan modellen och de platsbaserade uppskattningarna. Modellen som kördes med produkten från MOD13Q1, LAI i 250 meters cellstorlek, simulerade 78 % av den uppmätta variationen (R^2 = 0,73; p < 0,001) på samtliga undersökningsområden. Sammantaget så indikerar användande av PANEEx modell med 250 m vegetation en potential för framtida modellering i Arktis. Dataanalys genererade stora skillnader i modellerade NEE effekter och deras tillämpning i miljömodellering behöver därmed övervägas. Modellsimuleringar visar också potential att använda index vegetationsindex på en mycket finare skala, dvs. < 30 m för att fånga det arktiska heterogena landskapet.

Nyckelord: Arktis, netto ekosystem utbyte, index vegetation, ursprunglig satellitdata, stordata analys

Contents

1. Introduction

Concurrently, one of the most pursued topics in natural science is climate change (Kalnay et al., 1996; Francis, 2013) and its impact on carbon balance. High latitude regions contain substantial stores of carbon and the response of the Arctic carbon cycle to warmer conditions raises issues of a global concern (ACIA, 2005; McGuire et al., 2006; Tang et al., 2015). The notion that the Earth is warming every year (IPCC, 2014) is acknowledged in the scientific community, e.g. IPCC (Intergovernmental Panel on Climate Change) or ACIA (Arctic Climate Impact Assessment) monitor and reveal continuous evidence of climate warming (Chapman & Walsh, 1993). Studies of climate change suggest that Arctic regions are more profoundly affected by climate change relative to mid-latitudes (arctic amplification) (Screen & Simmonds, 2010; Serreze et al., 2009). The Arctic is more susceptible to environmental changes (e.g. increases in temperature) due to large number of positive feedback processes, involving snow and sea ice loss, land heat storage, etc. (Overland et al., 2015); thus it is regarded as a 'delicate' region.

The climatologically correct definition of the Arctic region (from the environmental perspective) can be derived from a natural phenomenon – the tree line, which indicates a zone where the severity of climate prevents trees from growing. However, a more common definition delineates all areas north of the Arctic Circle (66°32' N), which approximately marks the southern-most boundary of the midnight sun. Other studies have confined the Arctic according to the scope of their investigations; i.e. The Arctic Monitoring and Assessment Programme (AMAP) or the Circumpolar Arctic Vegetation Map (CAVM). All four definitions are used to evaluate the status of the Arctic in context of climate change, pollution, soil, etc. and produce public outreach reports to inform policy and decision-making processes.

Evidence for ecological changes on Arctic land can be gathered by (1) field-based measurements, (2) remote sensing and (3) long-term observations. Åkerman and Johansson have reported field measurements (1) on the state of the cryosphere throughout a 29-year period (1970s – 2006) (Åkerman, 1982; Johansson et al., 2008; Åkerman & Johansson, 2008; Christiansen et al., 2010). Their extensive research in the Nordic area, esp. northern Sweden, documents the changes in the active-layer thickness (top-most fluctuating seasonal soil layer), permafrost (subsurface earth materials remaining below 0°C for two consecutive years) presence and the effect of increasing temperatures. It is reported that the recent

climate-warming trend is thickening the active layer (2 cm/yr) and increasing permafrost temperatures, resulting in its decline (absence in 81% of sites) (Åkerman & Johansson, 2008). Field measurements based on local carbon balance are carried out using both gas chamber techniques (Williams et al., 2006) and eddy covariance (EC) towers (Baldocchi, 2003). These EC towers capture footprint upwind of the tower (see details in section 2.2.). Data obtained through remote sensing (2) is a relatively a new and effective way of measuring the environment (Faisal et al., 2012). Earth-orbiting satellites, such as MODIS (Moderate Resolution Imaging Spectroradiometer), LANDSAT (Land Remote-Sensing Satellite) or SPOT (Satellite Pour l'Observation de la Terre) provide remote measurements of the Earth's surface and atmosphere; the information derived from satellites is stored in geo-servers and is often available to the public (Zhao et al., 2013). Vegetation indices, i.e. leaf area index (LAI) and normalized vegetation index (NDVI) are typical satellite-derived products that provide information on vegetation phenology and composition of terrestrial ecosystems (Li et al., 2014). Despite the widespread use of LAI in science, it remains difficult to directly and indirectly quantify accurately, because of large spatial and temporal heterogeneity across the landscape (Van Wijk & Williams, 2005). Long-term observations (3) provide scientists information on climate through time series data (temperature, precipitation, etc. For example, ecosystem responses to climate and other changes can be observable on multi-decadal scales and hence, a long record of observations is necessary (Callaghan et al., 2013).

In modern science, researchers commonly conduct experiments through an interdisciplinary approach to understand natural phenomena from a more holistic approach. Combining knowledge from various fields of natural science, such as satellite remote sensing and environmental modelling can provide deeper insights into the impacts of climate change in a broader context (Comiso & Parkinson, 2004). The information provided by the satellite sensors consequently opens a broad field of implications within the Geo-physical science where *in situ* observations are often complemented by data acquired through remote sensing. Ecological parameters, such as gross primary production (GPP) or net ecosystem exchange (NEE) are examples of variables that can be computed via remote sensing based on existing empirical relationships and correlations (Mbufong et al., 2014).

1.1. Arctic net ecosystem exchange

GPP and NEE are utilized as ecological indicators to provide an approximation of the ecological state of a biome. NEE is a commonly used proxy that estimates carbon balance (carbon uptake vs. carbon release) in a particular area. Also termed net ecosystem production, NEE is defined as the residual difference between carbon uptake by vegetation GPP and carbon loss through autotrophic and heterotrophic respiration, collectively called ecosystem respiration (Kimball et al., 2009). In simpler terms, NEE is a useful measure of carbon flux between ecosystems and the atmosphere, such that:

$$NEE = (R_a + R_h) - GPP \qquad \text{(Equation 1)}$$

R_a – autotrophic respiration
R_h – heterotrophic respiration
GPP – gross primary production

There are a few denotations of NEE in various fields of science. In ecological terms, NEE is denoted as positive (+) and negative (-) where the signs refer to respective terrestrial loss or uptake of CO_2. A scientific site in Abisko, Sweden illustrates this with an average July NEE flux: -1.74 µmol m^{-2} s^{-1} (Stoy et al., 2013), i.e. an uptake of CO_2 to the terrestrial environment.

A study by Oechel & Vourlitis (1996) estimates carbon fluxes and suggests that vegetation distribution and landform patterns are indicators of carbon balance regimes at regional-scales. Mbufong et al. (2014) found that the understanding of the Arctic carbon exchange can be improved based on calculations of a simplified NEE model. The model utilizes parameters, the majority of which can be acquired or derived from remotely sensed data. Furthermore, based on the author's recent findings (Mbufong et al. (In Prep)), it was demonstrated that vegetation indices (digital datasets that describe the amount of greenness), such as LAI and NDVI, are crucial in modelling of carbon exchange in the delicate Arctic tundra. They have been identified as one of the major drivers of spatial variation of Arctic tundra NEE during the peak growing season (McMichael, 1999). Digital remotely sensed products, e.g. LANDSAT or MODIS that provide information about the distribution and density of vegetation throughout the Arctic have increasingly become available for scientific

use. Watts et al. (2014) employ MODIS Terra (MOD13A1) and Aqua (MYD13Q1) datasets to represent Arctic LAI and successfully simulate Arctic GPP.

1.2. Addressing problems with NEE calculation

Analysis of upscaled data, such as NEE over a large spatial extent and natural variation is a challenging task. Knowledge of NEE fluxes in the Arctic is constrained due to an uncertainty surrounding the accuracy of satellite images involved in the upscaling process (Williams et al. 2001). As previously stated, NEE estimations in the Arctic are linked with a representation of Arctic vegetation cover and other related proxies, e.g. LAI or NDVI. These vegetation representations are suitable for monitoring landscape patterns, however, they often provide generalized characterizations of Arctic biomes and therefore, they may contribute to distinct variations in modelled NEE. In general, the sensitivity of the satellite-derived estimations is closely linked to the technical configuration of a particular platform/sensor or to the method of acquisition (Stow et al., 1998). Therefore, the accuracy of modelled measurements depends on the quality of the input satellite data in the computation formula. Acquisition methods related to, e.g. spatial resolution, temporal resolution or spectral configuration of satellite sensors should be considered when selecting satellite-derived products. Spatial resolution refers to the pixel or cell size of images, ranging from coarse resolution (~1 km) to fine resolution (~10 m) (Longley, 2005).

Given vegetation properties are one of the major drivers of spatial variation of Arctic tundra NEE, different sources of LAI and NDVI are expected to yield variation in Arctic tundra characterization, and thereby, modelled NEE estimations may relate to the vegetation representations. Williams et al. (2001) demonstrate that LAI derived from satellites with spatial resolutions of approximately 1 km, related to the footprint of the EC flux data, show a poor correlation versus the *in situ* LAI in 0.2 m x 0.2 m quadrats. In conclusion, the authors propose that improved characterization of vegetation via remote sensing is required prior to any upscaling methods in carbon budgeting can reduce uncertainty in environmental modelling in heterogeneous landscapes.

In 2015, the Pan-Arctic Net Ecosystem Exchange (PANEEx), which was conducted by researchers at Lund University, Aarhus University and Dublin City University (funded by Google) developed a method to upscale remotely sensed data to refine understanding of

Arctic carbon fluxes in the terrestrial regions of Arctic tundra. The team used Google Earth Engine (GEE), an online interactive platform, which organizes geospatial information and makes it available for analysis to process data and generate results (Google Earth Engine Team, 2015).

In this thesis, I intend to introduce an approach that aids in reducing the knowledge gap between modelling of NEE and remote sensing. I propose the development of a method that utilizes remote sensing techniques and enables users to evaluate satellite-derived products and apply them in environmental modelling. Knowledge gained from this study can contribute to further development of large scale NEE models and reduce the uncertainty surrounding upscaling of satellite-derived data on a global scale.

1.3. Study purpose and aims

In section 1.2, the relevance of remotely sensed data and vegetation indices to modelling of Arctic NEE was described. Here, I present a study that improves the understanding in using satellite-derived products to model Arctic NEE using investigation of relationships between modelled and *in situ* measurements at 12 Arctic study sites. Thereby, this thesis aims to address the following goals:

- Acquire and apply vegetation indices from four MODIS products in the PANEEx NEE formula (Mbufong et al., 2015)
- Analyze the modelled NEE and LAI estimations and identify discrepancies or similarities in regards to ground observations
- Assess the effect of spatial resolution in determining the most realistic NEE estimations from MODIS products

It is assumed that the satellite-derived vegetation indices with finer spatial resolution may yield more accurate estimations of NEE in relation to *in situ* observations. Additionally, the temporal resolution (image acquisition interval) is also believed to be associated with precision of modelled NEE estimations because it defines the number of images used in the analysis. However, the analysis of LAI standard deviations illustrates that there is no significant variation in Arctic LAI during the studied period (31 days in July). The spatial and temporal resolutions of four MODIS-derived LAI inputs are outlined in table 1.

Table 1. Technical description of MODIS products used in this study.

Product	Spatial Resolution	Temporal resolution	Source
MCD15A3 - LAI	1 km	4 - day	LP DAAC, USGS*
MOD13A1 - NDVI	500 m	16-day	GEE, MODIS Terra
MOD13Q1 - NDVI	250 m	16-day	GEE, MODIS Terra
MYD09GA - NDVI	1 km	Daily	GEE, MODIS Aqua

* LP DAAC – Land Processes Distributed Active Archive Center

Recent developments in satellite remote sensing and environmental modelling offer users the potential for direct measurement and improved resolution of environmental constraints for estimating land-atmosphere carbon exchange (Kimball et al., 2009). Therefore, the first aim in this study is addressed by utilizing available data and employing appropriate software (e.g. Google Earth Engine) to generate four sets of Arctic NEE estimations based on four independent vegetation inputs. Employment of GEE as processing software is essential in this study because its cloud-based computational infrastructure can facilitate parallel processing of large quantities of data. The execution of the second and third aim is done based on statistical and graphical interpretations of the results. Here, the degree to which the four MODIS products describe the variation in NEE estimations at the study sites is examined. The configuration of MODIS products varies in this study and therefore, the results are assumed to reflect the suitability, advantages and disadvantages of each product used.

2. Theoretical Background

2.1. Carbon dynamics in the Arctic

Northern high-latitude boreal and tundra biomes play an important role in the global carbon cycle because they sequester a significant portion of atmospheric carbon dioxide (CO_2); they account for approximately 119 Pg of soil organic carbon (Kimball et al. 2009). Under current climatic conditions, the Arctic is regarded as a net sink of atmospheric carbon dioxide (IPCC, 2013), although there are large uncertainties surrounding the spatial variation of carbon fixation due to high heterogeneity across Arctic tundra. McGuire et al. (2010) discuss the culminating strength of the Arctic carbon land sink and argue that the diminished carbon storage over the terrestrial areas is due to increased fire disturbance. The authors

further emphasize that methane (CH_4) emissions are greater than the CO_2 sink, therefore the Arctic is a net source of greenhouse gas forcing to the climate system. Despite its low atmospheric concentrations, it is important to consider CH_4 because it has a substantially larger impact on the global warming potential than CO_2. Local wetting throughout the Arctic (Watts et al. 2012), in association with Arctic warming, may also increase the rate of CH_4 emissions, although a large uncertainty rests in the spatial variability of areas likely to get wetter or drier. In this thesis, however, the influence of CH_4 on carbon fluxes is not considered nor discussed.

Rapid changes in temperature of the northern latitudes relative to the mid-latitudes in recent decades are indisputable (Screen & Simmonds, 2010; Serreze et al., 2009). Since the pre-industrial era, the temperature anomalies associated with warmer climatic conditions over the Arctic have been unprecedented (IPCC, 2013). The impact of warming climate on terrestrial ecosystems (e.g. increased decomposition rates), particularly on the delicate Arctic has been increasingly becoming a subject of extensive scientific research. The sensitivity of Arctic ecosystems to climate (and anthropogenic) perturbations is well understood as the cryosphere, i.e. terrestrial snow and ice, permafrost and sea ice constitute major elements in global heat budget, however, scientists are often provided with little diagnostic insight about the underlying biophysical processes (Anderson, 2015). The assessment of possible consequences that northern ecosystems may experience is a challenging task, considering the region's landscape heterogeneity and the level of uncertainty amongst scientists. Recent studies (Piao et al., 2008; Angert et al., 2005 and Watts et al., 2014) demonstrate that current and projected regional warming trends may exacerbate global climate change by destabilizing regional soil organic carbon stocks and reducing the capacity of northern ecosystems to sequester atmospheric CO_2.

The projected changes associated with diminishing strength of carbon sink in the Arctic and the subarctic may inflict changes on the surface characteristics and may have further influence on vitality of circumpolar ecosystems, with considerable impact on plant and ecosystem carbon sequestration (Stiegler, 2016). Expanding our knowledge on geographical data and their acquisition is thus essential in gaining deeper understanding of carbon fluxes as well as developing more accurate models that simulate the prevailing dynamics in the Arctic. The development of ecosystem models (and estimations of sink/source areas in the Arctic) can offer a great potential for establishing an effective framework for high resolution

monitoring of greenhouse gases (CO_2) in the vulnerable changing Arctic. In order to accomplish these goals, further research and *in situ* observations are crucial for improved understanding of Arctic carbon dynamics.

2.2. Measurements of carbon in the Arctic

EC towers provide a valuable insight into the environmental constraints as they measure direct fluxes of CO_2 and CH_4 over the extent of ca. 1 km upwind of the tower (Baldocchi, 2003). Gas chambers represent another example of measuring carbon fluxes, although on a smaller scale (1 m x 1 m) and therefore, they capture a rather homogenous footprint of present vegetation (Williams et al, 2006). There are only a few sites that run gas chamber and EC tower measurements in the high Arctic. The limited availability of these measurements is closely linked to Arctic's harsh climate as well as to the remoteness of the stations (INTERACT, 2015). Certain measurements, e.g. plant annual productivity or maximum LAI require field sampling that can be conducted only without the presence of snow and, thus they are linked with Arctic climate seasonality. The datasets employed in this study therefore pertain to the peak season exclusively. July 1 - 31 is regarded as the time period of the maximum plant growth and also the time when the conditions where snow and moisture perturbations, as well as the surface self-heating effect, are expected to exert minimal or none impact on the instruments for EC measurements (Burba et al., 2008; Mbufong et al., 2014). Ground observations are scarce, but their amount in high and low Arctic is sufficient for scientists to assess results obtained through environmental modelling.

Knowledge on the various available vegetation products as well as their representativeness of the Arctic tundra has increasingly been becoming important for understanding the region's carbon balance dynamics. An accurate characterization of Arctic ecosystems can be achieved through remote sensing monitoring, which constitutes a key element for improving knowledge surrounding, e.g. climate change impacts, developments of more accurate models etc. To meet such demands, the environmental modelling community is working towards more accurate models, associated with both time (temporal resolution) and space (spatial resolutions). For instance, Watts et al. (2014) employ 16-day, 250 m NDVI to capture the overall seasonal variability in tower EC fluxes, whereas Tang et al. (2012) utilize 8-day, 500 m land surface reflectance to derive explanatory variables for

NEE estimation. Consequently, this demands powerful computation technology, advanced model development and evaluation techniques; the criteria depend on the type of application. Other organizations and institutes participate in conducting research of such scope, amongst which are, e.g. the Rossby Centre at Swedish Meteorological and Hydrological Institute (SHMI), Hadley Centre for Climate Prediction and Research or internationally recognized Google Earth platform as a part of Google Inc.

Investigating topics, such as NEE estimations based on various vegetation indices requires readily available data with, preferably, the finest resolution in time and space. Due to the wide range of applications and good data accessibility, MODIS products were chosen as an adequate source and representation of Arctic LAI (Table 1 in section 3.1. summarizes the major technical attributes of MODIS products used in this study).

2.3. Methodology in NEE Estimations

The modelling community uses a variety of models to determine carbon exchange. The models are parameterized based on functional relationships between ancillary variables that characterize the natural conditions. For instance, Williams et al. (2006) use the 'PIRT' model to determine NEE of CO_2 in tundra vegetation based on a combined representation of photosynthetic irradiance-response and temperature-sensitive respiration. They found moderately significant correlation between photosynthetic rate and LAI ($R^2 = 0.53$, $p < 0.01$). A simple terrestrial carbon flux model ('TFC') driven by satellite remote sensing inputs from MODIS and the Advanced Microwave Scanting Radiometer (AMSR-E) to estimate carbon stocks, NEE and respiration was developed by Kimball et al. (2009). GPP inputs in their study were acquired directly from a MODIS product (MOD17A2) and allowed successful computation of carbon stocks in high-latitude North America. The weakness in this method rests in a large spatial resolution of satellite-based GPP (1 km) and low accuracy of the TFC model to simulate dynamic equilibrium between GPP and ecosystem respiration.

Mbufong et al. (2014) found that light response curve (LRC) parameterization can be successfully used to predict summertime NEE of CO2 throughout the Arctic. Spatial variation of LRC parameters can be explained with leaf area index (LAI), mean July air temperature (Ta) and photosynthetic photon flux density (PPFD). PPFD is derived from

photosyntheticaly active radiation (PAR), which is an important element in ecological modelling (incident PAR spans in the visible spectrum from 400 to 700nm) (Liang et al., 2013). Such variables can be acquired through remote sensing with suitable spatial and temporal resolution, i.e. MODIS. Remotely sensed data are extensively used in Earth Science to monitor and analyze landscape changes on global and ecosystem scale (Luus et al., 2013). Using remote sensing techniques and Geographical Information Systems (GIS), it is possible to upscale satellite-based images by implementing Pan-Arctic Net Ecosystem Exchange (PANEEx) 2015 NEE formula (equation 2). This approach aims to effectively model estimations of carbon fluxes in the circumpolar Arctic. In this effort, an integration of environmental modeling with satellite data enables to gain further insights into climate change and its effects on terrestrial ecosystems on a large spatial scale.

The calculation of NEE in the pan-Arctic region based on freely available satellite and satellite-derived datasets will be implemented using the following relationship, utilizing the three stated variables (Mbufong et al, 2014):

$$\mathrm{NEE} = -(\mathrm{F_{csat}} + \mathrm{R}_d)\left(1 - e^{\frac{-\alpha(\mathrm{PPFD})}{F_{csat}+R_d}}\right) + R_d \qquad \text{(Equation 2)}$$

Where

- F_{csat} [µmol m^{-2} s^{-1}] indicates maximum CO_2 exchange at light saturation
- R_d or 'dark respiration' [µmol m^{-2} s^{-1}] represents nighttime CO_2 flux, i.e. when PPFD = 0
- PPFD [µmol m^{-2} s^{-1}] corresponds to the incoming solar radiation
- α signifies the initial slope of LRC. It can be also described as a parameter that affects the rate of CO_2 exchange in response to increase in PPFD.

3. Materials and Methods

The following section reveal characteristics of the study area, describe parameters used in NEE estimations, introduce satellite-derived products and they encompass the study design as well as statistical analysis.

3.1.Study Domain and study sites

This study estimates NEE for the Arctic, which encompasses regions, such as northern Alaska, North and Northeast Canada, Greenland, northern tip of Iceland, non-forested parts of Scandinavia and Northern Siberia (Figure 1). Due to environmental variations in, e.g. temperature, presence of large water bodies, permafrost cover etc., several definitions of the Arctic exist among scientists. The CAVM characterization of the Arctic was used to delineate to the boundary of the study area because its extent and biome classification are suitable for the purposes of this study, i.e. all study sites are included within the boundary. A Map of the study domain including the locations of the 12 study sites is shown in Figure 1. The southern limit of Arctic tundra vegetation is established based on the circumpolar Arctic vegetation map (CAVM, 2003). The following table (Table 2) identifies the studied stations that were used in the analysis. Some of the stations belong to the INTERACT (International Network for Terrestrial Research and Monitoring in the Arctic) network, which establishes 'hot spots' of research activity within the remote and vast environments (INTERACT, 2015).

Table 2. List of the studied sites in alphabetical order. The ecosystem type has been determined according to MODIS MCD12Q1 classification, International Geosphere-Biosphere Programme (IGBP).

Station	Location	Ecosystem type (IGBP)*	Latitude	Longitude
Anaktuvuk	Alaska	Open shrublands	68.93 N	150.27 W
Andøya	Norway	Grasslands	69.14 N	16.02 E
Barrow	Alaska	Permanent wetlands	71.32 N	156.63 W
Daring Lake	Canada	Open shrublands	64.87 N	111.57 W
Ivotuk	Alaska	Open shrublands	68.49 N	155.75 W
Kaamanen	Finland	Woody savana	69.14 N	27.30 E
Kytalyk	Russia	Open shrublands	70.83 N	147.49 E
Nuuk	Greenland, DE	Woody savana	64.13 N	51.39 W
Saymolov Island	Russia	Open shrublands	72.37 N	126.50 E
Seida	Russia	Woody savannas	67.05 N	62.93 E
Stordalen	Sweden	Woody savana	68.35 N	19.05 E
Zackenberg	Greenland, DE	Open shrublands	74.47 N	20.56 W

*Source: NASA, LP DAAC at https://lpdaac.usgs.gov

Data for analysis in this study comes from EC measurements of NEE of CO_2 and environmental variables, such as PPFD, temperature (air and soil), soil moisture, etc. Each station is equipped with meteorological instruments and EC towers for measuring turbulent heat and greenhouse gas fluxes between the biosphere and the atmosphere (Baldochi, 2003). Various instruments for EC measurements have been used across the study sites, such as the open-path LI-7500 (LiCor Inc., USA), closed-path LI-6262 and LI-7000 (LiCor Inc., USA) and the open-path IRGA designed by NOAA's Atmospheric Turbulence and Diffusion Division (ATDD). The usual flux footprint is defined as the area around the flux tower with the distance ca. 1 km. Footprint size depends, e.g. on the height of the EC tower, wind direction and speed and topography (Baldocchi 2003). Flux data in this study was based on eddy covariance data and is used as in *situ* NEE estimations across the study sites.

Eddy covariance technique ensures direct measurements of gas fluxes over larger regions compared to small-scale chamber techniques. EC measurements are thus appropriate for environmental modelling studies that consider ecosystem properties. Furthermore, this technique offers measurements of CO_2 flux over different times ranging from minutes to years (Mbufong, 2015). This study examines only peak season data (July, 2008 to 2010), which corresponds with the *in situ* NEE with a few exceptions (e.g. Barrow, Seida,) where missing data was complemented from previous or following consecutive seasons. The list of references for *in situ* NEE is located within Table 4.

The study sites are located within the most common types of tundra ecosystems throughout the circumpolar Arctic, with the latitudinal range 64 to 74° N (Mbufong et al., 2014). The ecosystems range from peat land to wet and dry tundra and certain sites (e.g. Barrow, Nuuk) exist on an underlying layer of continuous or sporadic permafrost (Callaghan et al., 2014). Due to a large spatial extent of the study domain, the climatic conditions vary significantly for each specific site.

According to Jensen & Rasch (2008), the low Arctic site Nuuk experiences a typical climate with mean annual Ta around 0°C and mean annual precipitation of ca. 700 mm (1961 – 1990). Williams et al. (2006) describe the annual mean Ta and annual precipitation at Barrow (high Arctic) between 1985 and 1993 as -7.4°C and 340 mm respectively. The vegetation can vary greatly, depending on the ecosystem type, from polar desert to spruce forest in the southern reaches of the low Arctic (Figure 1). The vegetation is dominated by sedges, low shrubs and tussock forming sedge; amongst the common species are *Eriophorum*

Figure 1. Map of studied domain. Polar conic projection shows 12 studied sites in global perspective. Different shades of blue denote Arctic bioclimatic subzones, according to zonation of Arctic vegetation (Matveyeva, 1998). The CAVM (Circumpolar Arctic Vegetation Map) line delineates the southern-most boundary of the Arctic, as used by CAVM Team, 2003. Note: since Fennoscandinavia is excluded from the official classification, the CAVM boundary has been re-edited according to the Arctic circle to integrate Swedish, Norweigan and Finnish sites.

Coordinate System: **CGS WGS 84**;
Projection: **North Pole Lambert Azimuthal Equal Area**.
Source: Author
Map was designed in GEE and ArcGIS

vaginatum, Vaccinium uliginosum, Betula nana, Salix spp., etc. (Kutzbach et al., 2007; Parmentier et al., 2011 and Rocha & Shaver, 2011).

3.2.Satellite-derived vegetation inputs

This study is based on investigating and applying various vegetation datasets to the PANEEx model (equation 2). Several vegetation index datasets were acquired from Moderate-Resolution Imaging Radiospectrometer (MODIS). Among the studied vegetation datasets are MODIS/MCD15A3 LAI, MODIS/MOD13A1 NDVI, MODIS/MOD13Q1 NDVI and MODIS/ MYD09GA NDVI. The metadata and supplementary information regarding the above-stated datasets was obtained from the Land Processes Distributed Active Archive Center (LP DAAC) site: https://lpdaac.usgs.gov/dataset_discovery.

The selection of the studied products was based on their different spatial and temporal resolutions as well as data availability. As mentioned, the remaining variables in the PANEEx model are PPFD (derived from PAR; PPFD = PAR × 4.57), and air temperature. Air temperature was estimated from MODIS land surface temperature (MOD11A1), as outlined in Mbufong et al., (in prep.) The MCD15A3 LAI product and its metadata for July 2008-2010 were obtained from https://lpdaac.usgs.gov/, maintained by the NASA Earth Observing System Data and Information System (EROS), USGS/EROS, Sioux Falls, South Dakota, 2014; the other three MODIS vegetation products are stored in readily-available format in GEE (Google Earth Engine Team, 2015), but originally were downloaded from USGS/EROS server as well. PAR data was obtained from The Global Land Surface Satellite (GLASS) server (Liang & Zhang, 2012). The GLASS PAR was available from 2008-2010 at 5 km spatial resolution and three-hour temporal resolution. Furthermore, this product had been evaluated and validated (Fang et al., 2013; Xiao et al. 2013a, 2013b) and the preliminary results indicate that they are of higher quality and accuracy than the existing product at eight-day temporal resolution (1982–2012 and 1981–2010) (Zhao et al., 2013).

Air temperature was derived from MODIS/MOD11A1 Land Surface Temperature and Emissivity, as used in Mbufong (2015), land surface temperature at 1 km spatial resolution and with a temporal resolution of one day. To preserve environmental conditions for each season, air temperature was derived separately for each July in 2008, 2009 and 2010. This means that every study site contains a specific air temperature measurement for a particular year. Additional subsets, e.g. clear sky coverage, day time and night time temperature

constitute MOD11A1. Data downloaded from MOD11A1 are contained within the GEE (Google Earth Engine Team, 2015).

The following sections provide a more detailed description of the MODIS vegetation products used in the analysis and, where applicable, steps taken in data preparation and harmonization:

- **MCD15A3, LAI**

MCD15A3 version 005 LAI/FPAR was acquired through the NASA-maintained server: https://lpdaac.usgs.gov. The data was downloaded using the USGS Global Visualization Viewer (GloVis).

The MCD15A3 V005 contains additional layers including: Fraction of Photosyntheticaly Active Radiation (FPAR), LAI and quality assessment data. Only layer 2 (LAI [m^2plant/m^2ground]) was used. MODIS LAI is available in multiple versions: MODIS Terra (MOD15A2), MODIS Aqua (MYD15A2) and the combined MODIS Terra & Aqua (MCD15A2) of the eight-day temporal resolution. The V005 combined MCD15A3 LAI (Terra & Aqua) is a product based on satellite image composites captured every four days. It was chosen for this study because of its global coverage, good accessibility and 1 km spatial resolution. More detailed metadata descriptions regarding LAI derivation were not provided by the source.

The increased temporal resolution is aimed at improved phenology monitoring and associated rapid changes that occur throughout the transition periods – plant bloom and senescence (Land Processes Distributed Active Archive Center (LP DAAC), 2002). This product represents LAI with the coarsest spatial resolution in this study and is therefore assumed to yield generalizations in modelled LAI and, consequently, a potential source of error in NEE estimations compared to *in situ* observations. MCD15A3 has not been incorporated to GEE database, therefore additional steps were required to input these raster data for further analysis:

1. *Append* individual image tiles to create East (E) and West (W) hemisphere Arctic LAI raster images. The LAI was separated into two halves as an extra step in order to circumvent downloading and handling large image files.
2. *Append* E and W raster images to form a global Arctic LAI.

3. *Cell statistics*-maximum pixel value to produce maximum LAI images for each July 2008-2010.
4. *Cell statistics*-mean pixel value to produce an average maximum Arctic LAI image for July 2008-2010.
5. *Clip* average maximum Arctic LAI to the study area (CAVN boundary, Figure 1.)

The terms highlighted in italics represent individual ArcGIS (10.2.2) tools used during the LAI data preparation.

- **MOD13A1, NDVI & MOD13Q1, NDVI**

MODIS datasets 13A1 and 13Q1, produced on 16-day intervals at multiple spatial resolutions, provide consistent spatial and temporal comparisons of vegetation canopy greenness, a composite property of leaf area, chlorophyll and canopy structure. The two datasets are derived from atmospherically-corrected reflectance in the blue, red, near-infrared wavebands, centered at 469 nm, 445 nm and 858 nm respectively (Didan & Huete, 2006). Despite the coarse temporal resolution, the composites 13A1 and 13Q1 are characterized by relatively fine pixel resolution, i.e. 500 m^2 and 250 m^2, making those suitable datasets for environmental modelling at regional and global scales. In this project, the environmental variation is sampled throughout the circumpolar Arctic and thus, the spatial scales of 13A1 and 13Q1 are expected to be sufficient. This approach should provide better insights into environmental modelling in the Arctic because other studies (McGuire et al., 2010; Watts et al., 2014) employ vegetation indices or vegetation classifications grids ranging from 0.5 - 1° (1° ~ 100 km). Furthermore, 13A1 and 13Q1 complements NOAA's Advanced Very High Resolution Radiometer (AVHHR), which provides high quality data acquisition and continuity in time series applications. This MODIS NDVI product is computed from atmospherically corrected bi-directional surface reflectances that have been masked for water, clouds, heavy aerosols and cloud shadows.

Given the adequate spatial and temporal dimensions of MODIS 13A and 13Q, it is presumed that these products likely yield the most realistic NEE estimations compared to measured values, considering the high variation of NEE fluxes in Arctic tundra (Tape et al., 2012).

- **MYD09GA, NDVI**

Originally, MYD09GA NDVI was generated from the MYD09GA MODIS surface reflectance composites. Its reflectance products provide an estimate of the surface spectral reflectance as it would be measured at ground level in the absence of atmospheric scattering or absorption. Cloud masking has been achieved using the 'state_1km' scientific dataset included in the MYD09GA NDVI product, which uses two cloud detection algorithms: the MOD/MYD35 cloud mask (Frey et al., 2008) and an additional, internal cloud screening (Vermote et al., 2008). The product's data quality has been validated at stage 2, i.e. the accuracy has been assessed over a widely distributed set of locations and time periods.

MYD09GA NDVI is delivered on daily basis, which makes it a suitable dataset in regards to vegetation dynamic representativeness, however, at the expense of pixel size (1 km^2). The fine temporal resolution and reduced atmospheric disturbance constitute MYD09GA a valuable product in this study and it is therefore presumed to provide sound NEE estimations. Hilker et al. (2012) successfully employ MYD09GA and derived composites (MYD09A1, MCD43A4 and MYD13A2) for observation of the vegetation dynamics in tropical environments like Amazonia where atmospheric disturbance (cloud aerosols, light scattering, etc.) is significant.

Portions of this description are modifications based on work created and shared by Google and used according to terms described in the Creative Commons 3.0 Attribution License (https://code.earthengine.google.com/).

3.3.LAI derivation

Leaf area index represents a good approximation of plant productivity in physical science. In general, it is defined as a dimensionless fraction of leaf area per ground surface area [plant m^2 / ground m^2], ranging from 0 (bare ground) to 10 (dense forest) (Myneni et al., 1997). Many publications deploy LAI to characterize the state of 'greenness' in their studies (Boelman et al., 2003; Van Wijk et al., 2005 Mbufong et al., 2014. NDVI is equivalent to LAI as both indices measure the amount of vegetation in an area, though NDVI is most likely to be associated with satellite-derived data because its calculation requires light reflectance data, i.e. red and infrared bands. It ranges from 0 to 1 and it is dimensionless, where 0 represents bare ground and 1 dense vegetation. Typically, data collectors measure

LAI in field using harvesting and scanning technique (leaf area / ground surface area) but MODIS NDVI is satellite-derived and has been a is stored as a digital dataset since February 2000. In order to calculate Arctic NEE based on PANEEx NEE formula, all vegetation inputs needed to be homogeneous, i.e. the satellite-derived NDVI products were converted to LAI. This is accomplished by implementing a relationship between LAI and NDVI, utilized by Van Wijk & Williams (2005) (Equation 3).

$$\mathrm{LAI} = 0.0026 \times \mathrm{e}^{(8.0783 \times NDVI)} \qquad \text{(Equation 3)}$$

LAI – leaf area index
NDVI – normalized difference vegetation index
e – exponent (Euler's number)

This relationship was developed to effectively derive LAI from NDVI in low vegetation Arctic tundra ecosystems nearby Abisko, Sweden. It was chosen because it successfully estimates 97% of the measured LAI through vegetation harvesting techniques. Moreover, the LAI estimation was conducted through combining field measurements of canopy reflectance (NDVI) and light penetration through the canopy. LI-COR LAI-2000 Canopy Analyzer (LI-COR, Lincoln, Nebraska, USA) was employed to carry out the measurement. Application of this relationship in this study is optimal because the parameters were calibrated mainly for the Arctic tundra environments.

The LAI of arctic vegetation could be estimated accurately and rapidly by combining field measurements of canopy reflectance (NDVI) and light penetration through the canopy (gap-fraction analysis using a LI-COR LAI-2000). By combining the two methodologies, the limitations of each could be circumvented, and a significantly increased accuracy of the LAI estimates was obtained.

3.4.Statistical approach

Similarly, data analysis in this study uses the conception of modelled vs. observed data and attempts to identify correlations and discrepancies between the two datasets. Thus, inferential statistics are used in order to make assumptions about the sampled data and to compare correlations of various sets of NEEs and LAIs (Lattin et al., 2003). A linear correlation line is fit through modelled and observed data in order to determine the amount

of explained variance, i.e. the goodness of fit (R^2), the root-mean-square-error (RMSE), the 95% significance test (p-value) and the regression line parameters (slope and y-intercept). The modelled data and ground observations are plotted on 1:1 scatter plots to assure clear data interpretation and comparison. Here, the slope parameter refers to the relationship between the modelled and measured data. For instance, given a plot with a slope of 0.5 means that the model simulated 50% of the measured fluxes; in other words, the slope of the correlation line describes the degree to which the model succeeded to yield estimations compared to *in situ* observations (ideally, the slope of a perfect fit would be 1, i.e. 100 %).

To effectively evaluate individual vegetation indices and their relevance to Arctic NEE estimations, it was necessary to exploit relationships between modelled and measured LAI and NEE scores separately. The LAI correlation analysis was carried out using 12 study sites whereas the NEE analysis contained only 11 sites; station Barrow was excluded from the NEE correlation due to insufficient data. The scope of analysis and calculation used in NEE upscaling is imposed by the techniques employed. Satellite derived data was retrieved and processed via Google Earth Engine (Google Inc.). ESRI ArcGIS Desktop vs. 10.2.2 (Redlands, CA, USA) was used for raster analysis and map generation and Matlab vs. R2014a (The MathWorks, Inc., Natick, MA, USA) served as a statistical processing software.

3.5.Data processing in Google Earth Engine

Prior to fitting a correlation line through the data, both NEE and LAI scores were calculated and retrieved using the GEE server (GEE, Google Inc.). GEE encompasses other extensions, such as Google Maps Engine (GME) that allows users to upload external geographical data in form of raster files, vectors, etc. and makes them compatible with GEE interface. The connection of external variables with GEE is facilitated using an ID linker code so the dataset can be directly imbedded in PANEEx NEE model on the same platform. Using Java syntax, which is GEE's operational input language, a model script that links all corresponding variables and processes has been developed, as outlined in workflow chart (Figure 2); The boxes with green outline are identified as the main three input variables (air temperature Ta, LAI, and PAR) in NEE estimation. The main three input variables were used to define the LRC parameters (explained in section 2.3.) F_{csat}, α and R_d, as outlined in

Mbufong et al. (2014). Ta is used to define F_{csat}, PAR is used to derive PPFD and LAI is used to define all three parameters, i.e. F_{csat}, α and R_d. As mentioned, the various NEE estimations were obtained based on alternations of vegetation proxy datasets, i.e. the model was run four times and each iteration, a LAI proxy was substituted with one of the MODIS LAI/NDVI products described in section 1.3, Table 1.

It was also necessary to upload external data into GEE to perform the analysis. In this study, a vector file containing XY coordinates of *in situ* sites had been manually ingested into GEE via GME. The ingested vector that spatially coincides with the coordinates of ground observation stations and EC towers was used for LAI and NEE score extraction. This ensured that the location of extracted modelled and *in situ* data was matching. Geospatial

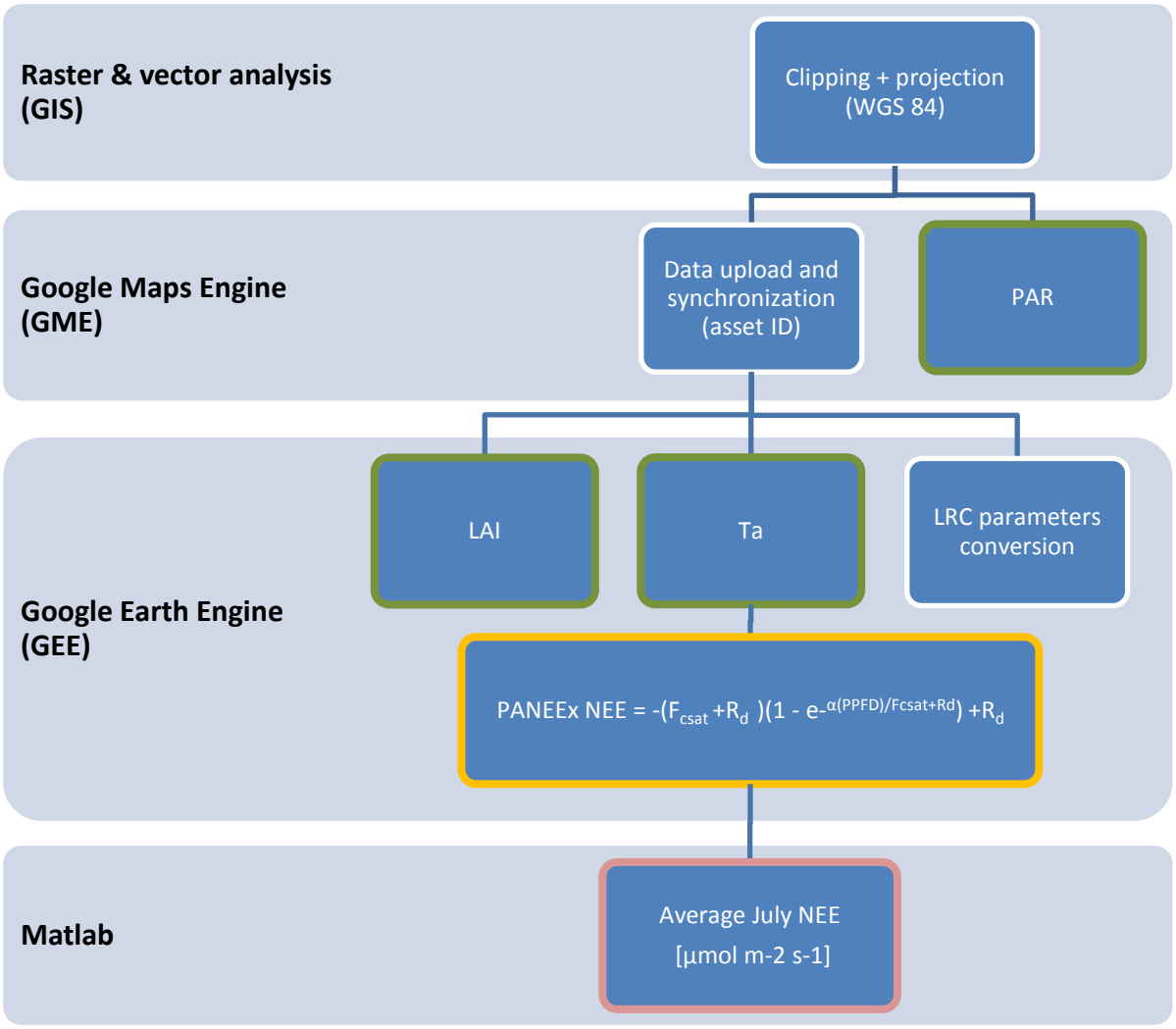

Figure 2. Workflow chart of NEE calculation. The chart displays chronological steps in data processing as well as **input** data in the PANEEx NEE **formula**, based on Mbufong (2015). The final **product** represents an average daily carbon flux at the peak of the growing season in [µmol m^{-2} s^{-1}].

tools included in GEE allowed pixel extraction based on XY coordinates, masks and fusion tables; additional external data, i.e. PAR and vector files that are not included in GEE database were uploaded and synchronized through GME.

Analysis of global datasets is a demanding task in terms of data storage and operational speed. Data processing in GEE presented an effective way of handling large datasets in this study because the analysis was executed through a Google-powered cloud server, which enables simultaneous operations at a time. The execution of the PANEEx script in GEE does not have any effect on the precision of the produced estimations. There are a few constraints associated with GEE, i.e. time and the methods used. Large datasets can be processed by GEE if the network is not overloaded; in other words, the processing time is related to the size of the dataset being processed and the current server workload.

3.6.Execution of PANEEx in Google Earth Engine

Carbon fluxes in the Arctic are regarded as fluctuating proxies that are closely linked with variations in ambient topography and climate conditions. Although there are clear patterns in carbon flux dynamics in the Arctic, studies (Lund et al., 2012; Mbufong et al., 2015) have shown that the correlations between ancillary natural processes and CO_2 uptake or release have a non-linear nature. For instance, light availability and length of the growing season are both related to plant GPP in a particular year. In this study, multiple linear relationships between the LRC parameters and satellite-derived variables are implemented, i.e. Ta and LAI to estimate carbon exchange. Modelling of NEE estimations throughout the circumpolar Arctic is contingent on the three listed variables, particularly the PAR, owing to its substantially fine resolution in time (8 times per day). PANEEx NEE model is therefore a function of PPFD (derived from PAR) in [W/m^2].

In high-latitude areas where PPFD images were aligned imperfectly (at the expense of seam lines), a hollow space in form of masked pixels containing no data was substituted with pixels, such that PAR = 0 W/m^2. This resulted in a potential source of error and will be further discussed (see section 5.2.2).

Given the study scope of 31 days in July of each study year, the model produced 31 daily NEE outputs based on three-hour temporal resolution of PAR. Averaging the 31 NEE daily estimations in July for each study year has resulted in deriving an average July NEE where this measurement is considered as a total annual carbon yield for a particular year. The

highest photosynthetic rate by plants was considered at full vegetation growth. This was achieved by implementing maximum LAI raster images to account for the potential plant production at light saturation. Maximum LAI means that that the highest pixel value throughout the 31 days was prioritized instead of a monthly mean during a raster overlay analysis.

The PANEEx NEE model was executed for three separate years (2008, 2009 and 2010) and the presented results show a single NEE average for this time period. After the PANEEx model had quantified Arctic NEE, MATLAB and ArcGIS were used for further data analysis and figure generation.

4. Results

The following chapters analyze the relationships between modelled and observed LAI and NEE scores for the study sites. The results are illustrated in 1:1 scatter plots, bar graphs and supplementary maps. Linear correlations and parameters slope and y-intercept are used to infer about the statistical significance and relationship strength between modelled and in situ data.

4.1.Satellite-derived LAI

The satellite-derived vegetation indices compared to ground measurements are presented in this section. Prior to analyzing the modelled NEE estimations, the LAI scores from the four MODIS products were plotted against in situ observations in attempts to identify their capability to describe vegetation variation amongst the studied sites. Figure 3 illustrates linear correlations between satellite-derived and *in situ* LAI scores (n = 12). It was found that MODIS products yielded relationships with slopes ranging from slopes 1.22 to 2.45 and RMSE spanning between 0.12 - 0.29. This shows that the satellite-derived products contributed with a systematic bias ranging from 22 % to 145 % with respect to *in situ* LAI. In spite of the bias in calculated LAI, all four MODIS products yielded relationships that satisfy the 95% significance test. Very strong relationships between satellite-derived and ground LAI were achieved using datasets (MCD15A3 and MOD13A1) shown in Figure 3, plots A) and B), R^2 = 0.8 and 0.89 respectively. In both cases, however, the LAI was considerably overestimated (slopes: 2.45 and 1.47 respectively).

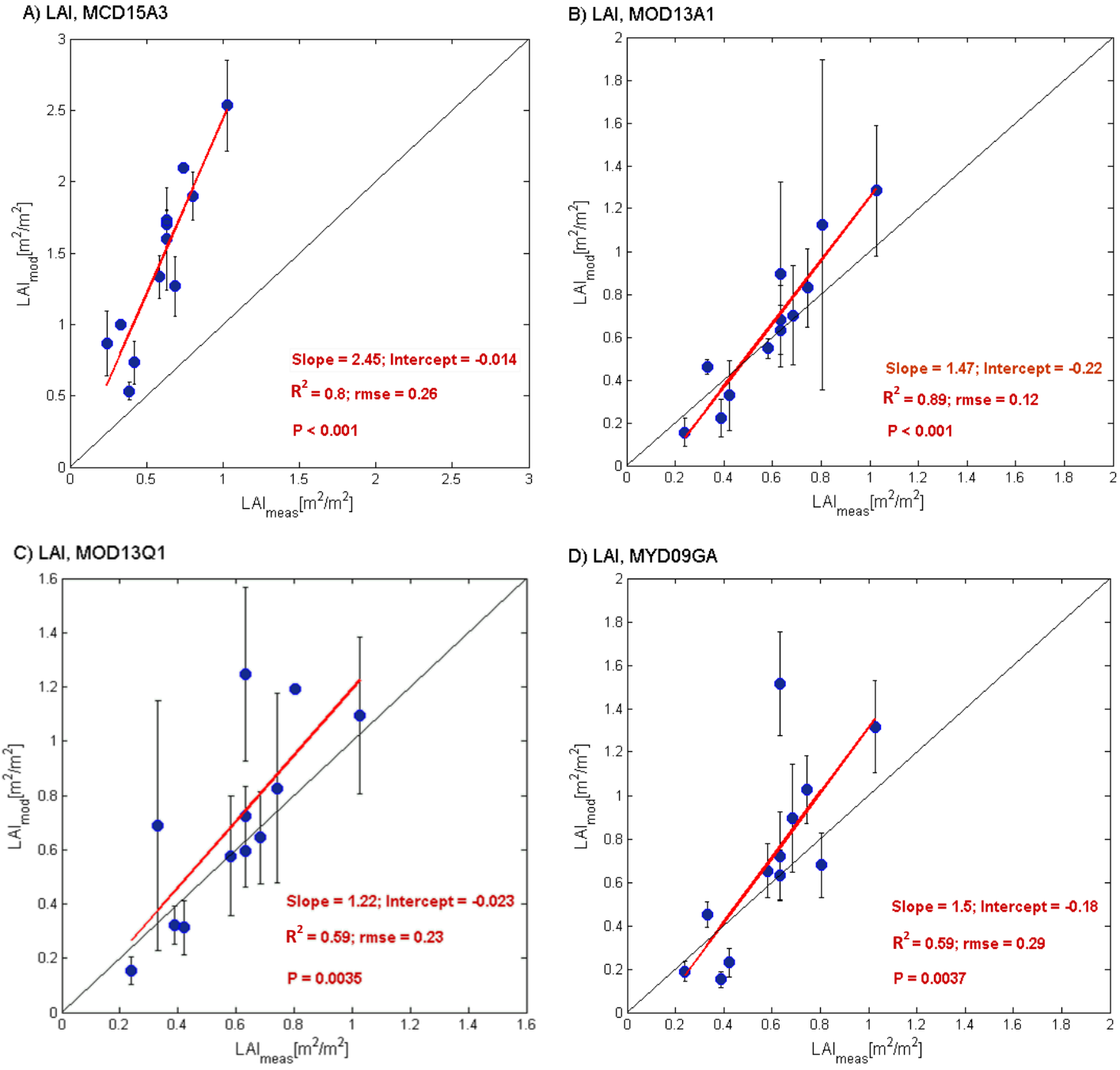

Figure 3. Linear correlations between satellite-derived and *in situ* maximum average July LAI for 12 Arctic sites. Maximum average LAI refers to the mean of the three maximum LAIs in 2008, 2009 and 2010. Maximum LAI is the highest measured value in July in a particular year. The concept of maximum LAI is used in order to simulate the potential gas exchange at peak-season (full vegetation growth).

Table 3. Average maximum July leaf area index in [m^2/m^2] acquired from four MODIS products: satellite-derived vs. *in situ*. The listed LAI scores were derived from NDVI according to methodology used in van Wijk & Williams (2005).

Study sites	MCD15A3 LAI	σ	MOD13A1 LAI	σ	MOD13Q1 LAI	σ	MYD09GA LAI	σ	Measured LAI	σ
Anaktuvuk	1.73	± 0.06	0.63	± 0.11	0.59	± 0.13	0.72	± 0.2	0.63	± 0.0031
Andøya	2.10	± 0	0.83	± 0.18	0.83	± 0.35	1.02	± 0.16	0.74	± 0.0042
Barrow	0.73	± 0.15	0.33	± 0.16	0.31	± 0.1	0.23	± 0.07	0.42	± 0.0026
Daring Lake	1.00	± 0	0.46	± 0.04	0.69	± 0.46	0.45	± 0.06	0.33	± 0.0028
Ivotuk	1.90	± 0.17	1.13	± 0.77	0.63	± 0.01	0.68	± 0.15	0.81	± 0.033
Kaamanen	1.27	± 0.21	0.70	± 0.23	0.64	± 0.17	0.9	± 0.25	0.69	± 0.033
Kytalyk	1.60	± 0.36	0.68	± 0.16	0.72	± 0.11	0.63	± 0.12	0.63	± 0.033
Nuuk	1.33	± 0.15	0.55	± 0.05	0.58	± 0.22	0.65	± 0.12	0.58	± 0.0028
Saymolov Isl.	0.53	± 0.06	0.22	± 0.09	0.32	± 0.07	0.15	± 0.04	0.39	± 0.0039
Seida	2.53	± 0.32	1.28	± 0.3	1.09	± 0.29	1.32	± 0.21	1.03	± 0.0026
Stordalen	1.70	± 0.1	0.89	± 0.43	1.25	±0.32	1.51	± 0.24	0.63	± 0.0031
Zackenberg	0.87	± 0.23	0.15	±0.07	0.15	± 0.05	0.19	± 0.05	0.24	± 0.0039

Furthermore, the dataset MOD13Q1 (Figure 3C) represents the least biased relationship in this study (slope: 1.22). In contrast, it accounts for the lowest correlation fit (R^2 = 0.59, RMSE = 0.23). LAI scores for all study sites and four MODIS products are reported in Table 3. The standard deviations (σ) for MCD15A3, MOD13A1, MOD13Q1 and MYD09GA span between 0 to ± 0.36, ± 0.04 to ± 0.77, ± 0.01 to ± 0.46 and ± 0.04 to ± 0.25 respectively.

Results from table 3 are graphically presented in a bar chart (Fig. 4). The colored bars represent satellite-derived LAI scores from four MODIS products and the bar whiskers correspond to the standard deviation, i.e. the annual variation in July LAI throughout the study period 2008 – 2010 LAI. This figure presents a quantitative comparison of satellite-derived and ground LAI scores for each study site. The performance and accuracy of each MODIS product can be compared to the *in situ* LAI displayed as a 'blue dot'. The results from this figure suggest that MCD15A3 has yielded LAI estimations that exceed the *in situ* measurements by a factor of two and, in case of a high Arctic site Zackenberg, by a factor of three. Therefore, it is considered as the least suitable satellite-derived product. Moreover, the products MOD13Q1 and MOD13A1 demonstrate the most realistic representations of the *in situ* measurements, both graphically and statistically (see the statistical parameters in Figure 3).

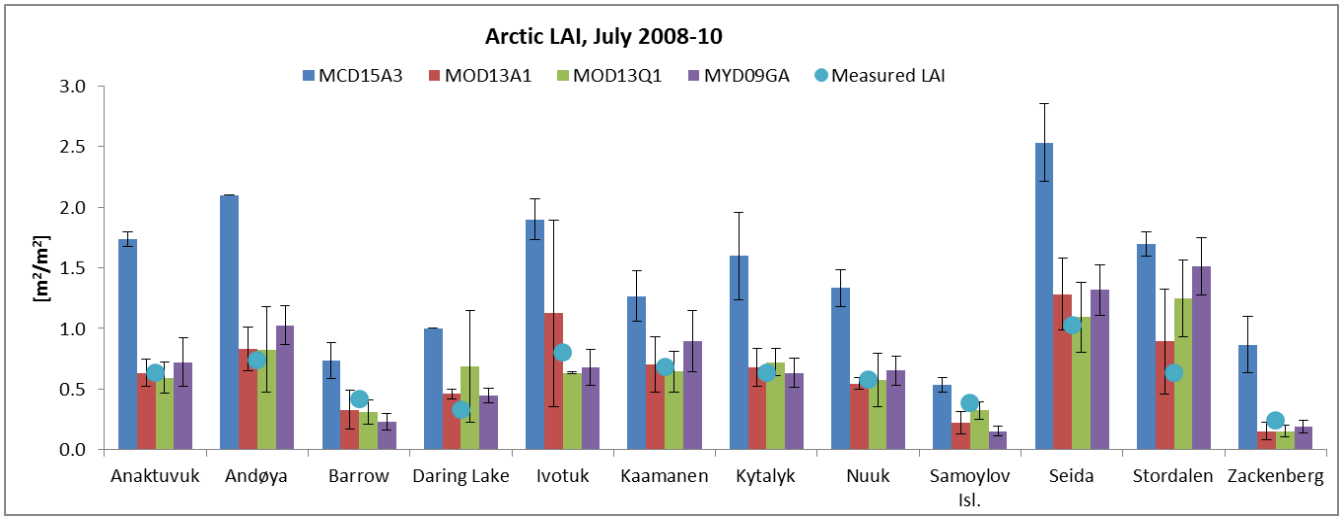

Figure 4. Graphical representation of the Arctic satellite-derived and ground LAI scores at the 12 study sites. The error bars denote the standard deviation of LAIs between 2008-2010.

4.2.Satellite- derived NEE

This section presents modelled daily peak-season NEE based on different LAI inputs. Figure 5 illustrates relationships between modelled and measured NEE at the study sites (n = 11). It was found that 1 out of 4 vegetation datasets (MCD15A3) yielded NEE estimations that poorly correlated with the variation contained in *in situ* data (R^2 = 0.24, n = 11). The linear correlation further showed that the residuals account for a large variation and the data falls out of the 95% significance interval ($p < 0.72$) (Fig. 5A). A successful representation of Arctic NEE was achieved by implementing MOD13Q1 (Fig. 5C), which estimated 78% of the measured fluxes (slope = 0.78) with RSME = 0.22. There is strong fit between MOD13Q1 NEE and *in situ* (R^2 = 0.73, n = 11), though it is consistently underestimated throughout all the sites.

In spite of having the second finest spatial resolution (pixel size = 500 m), MOD13A1 has not succeeded to effectively characterize the NEE (outside of the significance interval, $p < 0.079$); a boxplot analysis of modelled NEE based on MOD13Al (see Appendix 2) had identified an outlier Seida. In this case, the outlier was treated as confounding data and was accounted for in the analysis; however, its exclusion from the linear correlation did not improve the fit (Fig. 5B). The other three NEE datasets did not account for any outliers. MYDGA09 NEE showed a moderate goodness of fit compared to *in situ* (R^2 = 0.52, n = 11) (Fig. 5D) with RMSE = 0.34 and is, as well as MOD13Q1, consistently underestimated throughout the Arctic study sites (slope = 0.86). In this study, MYDGA09 NEE therefore constitutes the second most suitable estimation, even though it had been initially assumed that its relatively coarse spatial resolution (1 km) may not generate the expected outcomes. Although one outlier (Seida) was identified within the modelled NEE sets, other NEE estimations (e.g. Barrow) had to be excluded from the analysis due to insufficient data or errors related to the reflectance properties in satellite-derived products.

Modelled and measured NEE scores, including the standard deviation for all sites are reported in table 4.

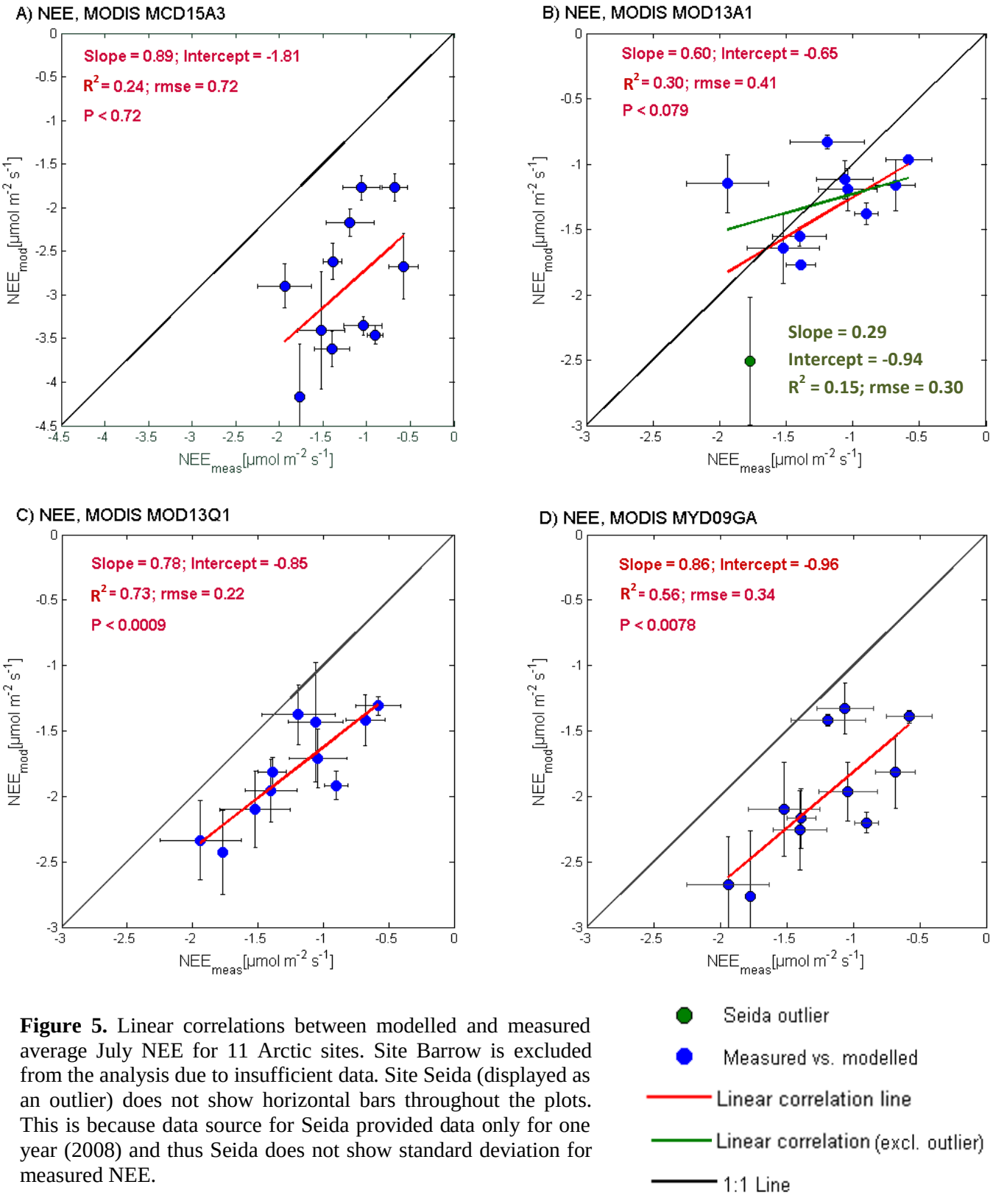

Figure 5. Linear correlations between modelled and measured average July NEE for 11 Arctic sites. Site Barrow is excluded from the analysis due to insufficient data. Site Seida (displayed as an outlier) does not show horizontal bars throughout the plots. This is because data source for Seida provided data only for one year (2008) and thus Seida does not show standard deviation for measured NEE.

Table 4. Average July net ecosystem exchange fluxes in [µmol m^{-2} s^{-1}]: measured vs. modelled. The modelled fluxes were calculated based on the listed MODIS products. The average period for modelled fluxes is July 2008 – 2010. Note: The reported negative values indicate uptake from the atmosphere by land. Site Barrow is excluded from the analysis due to insufficient data.

Study sites	MCD15A3 NEE	σ	MOD13A1 NEE	σ	MOD13Q1 NEE	σ	MYD09GA NEE	σ	Measured NEE	σ	Measured NEE Reference
Anaktuvuk	-3.46	± 0.11	-1.92	± 0.082	-1.38	± 0.11	-2.2	± 0.08	-0.9	± 0.09	Rocha & Shaver (2011)
Andøya	-3.62	± 0.20	-1.96	± 0.07	-1.56	± 0.24	-2.26	± 0.30	-1.4	± 0.2	Lund et al. (2015)
Daring Lake	-1.77	± 0.14	-1.43	± 0.15	-1.12	± 0.46	-1.33	± 0.19	-1.06	± 0.21	Lafleur & Humphreys (2008)
Ivotuk	-3.35	± 0.11	-1.71	± 0.16	-1.2	± 0.22	-1.97	± 0.22	-1.04	± 0.22	Kwon et al. (2006)
Kaamanen	-2.62	± 0.2	-1.81	± 0.03	-1.77	± 0.11	-2.17	± 0.23	-1.39	± 0.11	Aurela et al. (2004)
Kytalyk	-3.4	± 0.68	-2.1	± 0.27	-1.64	± 0.29	-2.1	± 0.36	-1.52	± 0.27	Parmentier et al. (2011)
Nuuk	-2.17	± 0.15	-1.38	± 0.05	-0.83	± 0.23	-1.42	± 0.05	-1.19	± 0.28	Westergaard-Nielsen et al. (2013)
Saymolov Isl.	-1.77	± 0.16	-1.42	± 0.20	-1.16	± 0.2	-1.81	± 0.28	-0.68	± 0.15	Kutzbach et al. (2007)
Seida	-4.17	± 0.61	-2.43	± 0.49	-2.51	± 0.32	-2.77	± 0.5	-1.77	--	Maruschak et al. (2013)
Stordalen	-2.9	± 0.25	-2.34	± 0.22	-1.15	± 0.30	-2.67	± 0.37	-1.94	± 0.31	Christensen et al. (2012b)
Zackenberg	-2.67	± 0.38	-1.31	± 0.02	-0.96	± 0.07	-1.39	± 0.05	-0.58	± 0.17	Lund et al. (2012)

The bar chart (Fig. 6) graphically illustrates the NEE fluxes contained in Table 4. The colored bars represent modelled peak-season NEE based on four MODIS products and the bar whiskers correspond to the standard deviation of NEE throughout the study period 2008 – 2010. The figure depicts the contribution of MODIS products to NEE estimations at each study site; the 'blue dot' (measured NEE) serves a comparison of what the modelled NEE should be equivalent to. A visual analysis suggests that the NEE estimations generated from MCD15A3, MOD13Q1 and MYD09GA are consistently overestimated at all 11 study sites, with the standard deviation (σ) ranging from ± 0.11 to ± 0.68, ± 0.07 to ± 0.46 and ±0.05 to ± 0.37 respectively, whereas vegetation dataset MOD13A1 contributed to overestimations at 9 study sites with the seasonal variation, i.e. σ = ± 0.02 to ± 0.49. Alternatively, an overestimation in NEE means that the Arctic tundra behaves as a pronounced sink of CO_2 compared to reality. In other words, the model has simulated that the net CO_2 uptake by land is greater than the *in situ* observations suggest in this study.

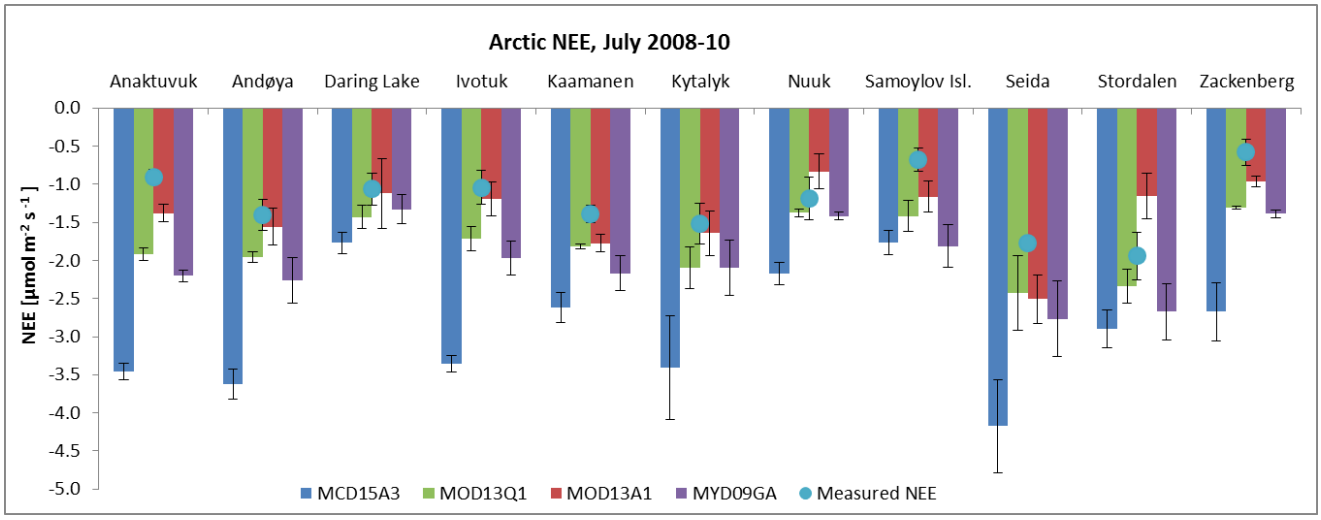

Figure 6. Graphical representation of the Arctic modelled and measured NEE fluxes at the 11 study sites. The error bars denote the standard deviation of NEE between 2008 - 2010. Site Barrow is excluded from the analysis due to insufficient data.

4.3.Examples LAI variation on small scale

Two study sites, i.e. Stordalen (Sweden) and Zackenberg (Greenland, DE) were chosen as examples to illustrate small-scale variation in satellite-derived LAI. In order to show the differences between the four MODIS products, a map with zoom-in windows of 5 x 5 km was produced (Fig. 7). The eight windows present characteristics of the four satellite-derived

LAI raster images at the two study sites. The differences between the LAI representations reflect mainly the spatial resolutions of the MODIS products but also the configuration of the satellite sensors. A particular level of pixel patchiness is evident as the MODIS products capture Arctic vegetation variation at spatial resolutions ranging from 1 km to 250 m. A visual analysis of the LAI maps shows that MOD13Q1 LAI (Fig. 7C) characterizes the landscape with the highest level of detail. The other products, Fig. 7A, 7B and 7D, present Arctic LAI in a coarser resolutions and their representativeness of this diverse land raises an uncertainty; as it was emphasized earlier in this study, Arctic landscape often varies on much smaller scale.

Another unique characteristic of the various MODIS products is their ability to discriminate and classify non-vegetation land cover classes, i.e. to distinguish between water bodies, bare ground etc. This is especially important for sites with a close vicinity to coastlines or lakes. Figure 7 shows that all MODIS products capture the land cover heterogeneity on different scales. For instance, Stordalen is situated directly south of the lake Torneträsk. As seen in Figure 7A and 7D, this is demonstrated only by two MODIS products (MCD15A3 & MYD09GA) which identify a water body in the same location and extent; the other products show several sporadic pixels classified as ‘water bodies’ (Fig. 7B) or show no presence of water at all (Fig. 7C). This potentially questions the accuracy of MODIS products nearby wetted areas in this study. As demonstrated in the previous chapter, MCD15A3 has not contributed to sound NEE estimations compared to in situ, however, its features enable users to distinguish between LAI and other general land cover classes.

The value of the underlying incident LAI pixel can be seen in the green patches (Fig. 7) and compared to in situ measurements noted in the figure description. Pixels in images of larger resolutions are expected to be associated with generalizations, however, in areas of low landscape heterogeneity, they can provide similar or the same LAI approximation as the finer pixels.

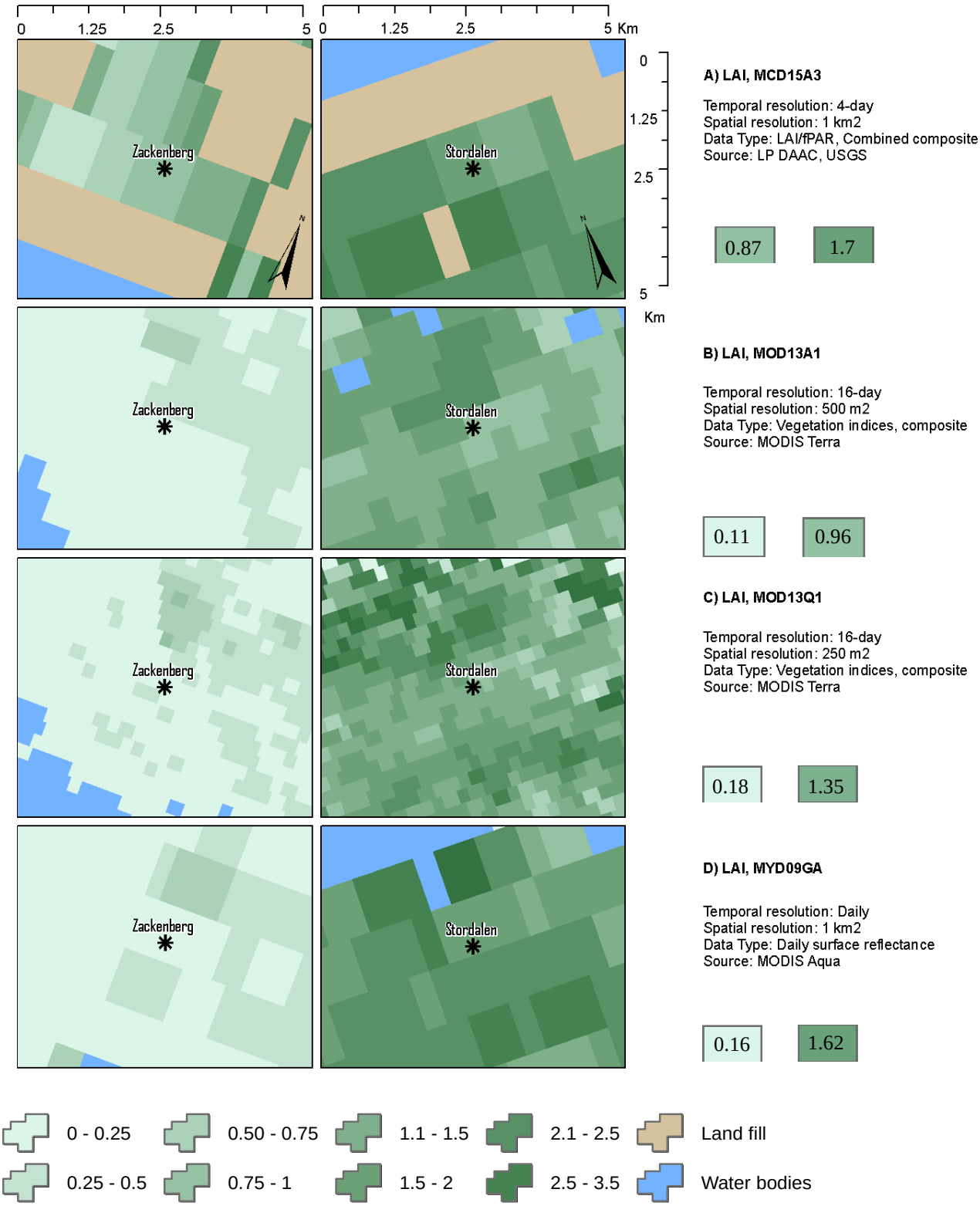

Coordinate System: CGS WGS 84;
Projection: North Pole Lambert Azimuthal Equal Area.
Source: author

Figure 7. Examples of small-scale variations in MODIS LAI products for 2 study sites: Stordalen and Zackenberg. Paired images A) to D) correspond to individual MODIS LAI datasets and illustrate 'patchiness' of LAI gridcells in 5 x 5 km window. Values in green-shaded rectangles represent the underlying satellite-based LAI value for each study site. This can be compared to *in situ* LAI, where: Zackenberg ~0.24 and Stordalen ~ 0.63

5. Discussion

5.1.Suitability of MODIS products

The results suggest that the alternation of MODIS products in PANEEx 2015 model accounts for considerable variation in the modelled NEE throughout the Arctic. It was demonstrated, that MOD13Q1 (250 m) provides the most realistic NEE estimations followed by MYD09GA (1 km). This is in agreement with Schubert et al. (2012) who modelled Nordic GPP using MODIS time series data. They report that 250 m MODIS vegetation products captured the overall seasonal variability in tower EC flux records better than the MODIS 1 km GPP product. Furthermore, Watts et al. (2014) also employ 16-day 250 m NDVI scores in satellite driven modelling of carbon fluxes throughout the Arctic. Interestingly, they used combinations of MODIS Terra (MOD13A1) and Aqua (MYD13Q1) records, which reduced the acquisition interval gap to approximately 8 days, compared to 16 days as used in this thesis. By combining two MODIS products, the authors managed to improve the temporal resolution of NDVI by ca. 50% (acquisition interval was halved). Their NEE simulations showed a strong correlation ($R > 0.80$, $p < 0.05$) with tower EC records. This finding suggests that 250 m MODIS vegetation products used in this study present a very suitable datasets for NEE estimations and are in accord with other studies. As further shown in Watts et al. (2014), higher temporal resolution is beneficial and can improve the overall accuracy of the modelled NEE and LAI estimations by combining multiple MODIS products. The authors used linear interpolation in order to fill in the missing data and reduce the acquisition interval. However, this constitutes an additional step in data analysis and the method may introduce a source of error (Meijering, 2002)

Another study performed by Stow et al. (1998) implements satellite-derived NDVI and cover type maps to estimate CO_2 flux in Arctic tundra. Here, a coarse-scale NDVI from NOAA AVHRR (ca. 1 km) and SPOT (20 m) are used to extrapolate regional CO_2 fluxes with a particular emphasis on landforms and spatial patterns. It was found that 1 km NDVI is much larger than the resolution of the landscape features, whereas SPOT-generated relationships established at 1-10 m suggest that NDVI is a good predictor of CO_2 exchange (McMichael, 1999). Moreover, the authors state that even at the 20 m sample scale, the fine landscape features influence the NDVI variability.

Several implications are proposed from the above claims to the methods in this thesis. (1) Satellite-derived vegetation indices are valuable proxies in environmental modelling, but

their effectiveness in modelling of Arctic vegetation varies on the scale and type of application. (2) Coarse-scale vegetation indices (< 1 km) may be useful in planet-scale modelling, but are too coarse for regional NEE estimations and (3) even 250 m vegetation indices may present an uncertainty. The latter is debated in Tape et al., (2012) who argue that modelling in environments with distinct landscape heterogeneity, 500 m and 250 m vegetation indices may not be sufficient. It is further reported that the landscape heterogeneity varies greatly throughout the Arctic and the "patchiness" of NDVI may be underestimated or overlooked due to a large pixel size.

5.2. Accuracy of modelled NEE and LAI

5.2.1. Methods-related uncertainty

There are potential sources of uncertainty in the study methods that may have introduced errors in the modelled NEE and LAI scores. The accuracy of these estimations is constrained by the limited number of *in situ* observations in this study. It is important to emphasize that carbon fluxes are studied on regional as well as global scale and therefore, the requirements on validation sites may vary.

First, the number of sites in this study (n = 12) did allow statistically significant analysis and verification of modelled results against ground observations in most cases. In comparison, research demonstrates that moderately correlated measurements of carbon fluxes in global Arctic were carried out by using only 9 study sites (Kimball et al., 2009). The correspondence of modelled NEE and *in situ* measurements in their investigation accounted for between 26% and 50% of *in situ* variability for boreal sites and less than 28% of *in situ* variability for tundra sites. In regional scale, McMichael (1999) examined the GPP-NDVI relationship at two Alaskan tundra sites, approximately 200 km apart, with 12 – 16 observations for each plot. The NDVI accounted for 68% and 74% variation of the NPP at the confidence level $p = 0.02$.

Compared to the aforementioned studies, the CO_2 fluxes at certain ecosystems may be underrepresented in this study. The results presented in this thesis could be improved by incorporating more *in situ* measurements. Locations, such as Svalbard, Norway or Iceland are not included in this work and would be a valuable contribution to the rest of the study sites in terms of balanced proportion of ecosystem extents.

Secondly, the sources of error can be due to imperfect relationships between variables, e.g. the methods of LAI derivation. *In situ* NDVI measurements in this study have been sampled by many field collectors using various instruments and non-standardized techniques. Furthermore, the NDVI scores needed to be converted to LAI scores, to which PANEEx 2015 model is calibrated. Having employed the Wijk & Williams (2005) relationship, the LAI was derived from NDVI, explaining 97 % of the NDVI variation. Although this relationship enables effective NDVI-LAI conversion, it is imperative to stress that this model has been designed in low vegetation ecosystems nearby Abisko, Sweden and thus, the estimation of LAI scores throughout the low and high Arctic generates a source of error and needs to be considered. This can be seen in relatively high standard deviations (e.g., σ for MOD13A1 = 0.77) for and maximum to minimum ranges of modelled LAI scores in this study. In comparison, Fang et al. (2013) cover an extensive study on MODIS LAI and claim that non-forested regions account for a typical deviation less than 0.5.

The product MCD15A3 is the only LAI source in this study and hence, needed not to be converted to NDVI. According to the produced plots, this product contributed to large biases in of both LAI and NEE estimations. This could be because LAI used herein is more sensitive to vascular plant cover, thus ignoring non-vascular understory like mosses and lichens, which contribute significantly to Arctic ecosystem CO_2 exchange (Street et al., 2012).

The contribution of various temporal resolutions of MODIS products is not discussed in depth in this study, although its effect in combination with spatial resolution can be discerned between 4-day MCD15A3 and 16-day MOD13A1 LAI estimations (Figure 3A) and 3B)). Here, the 4-day product with finer temporal resolution shows lower variability (standard deviation bars) throughout the study years as opposed to the 16-day product. This finding may be attributed to the inability of the 16-day product to simulate landscape variation during the study period, resulting in greater differences in satellite-derived July LAI estimations. The relatively large patchiness of 1 km MCD15A3 LAI could explain the shorter span of the standard deviations in satellite-derived LAI estimations. The cell size of 1 km with combination of 4-day acquisition time constitute MCD15A3 a valuable product that delivers stable estimations with a low variation spread. The weakness of this product rests in its spatial resolution that may not be sufficient to capture the resolution of landscape features in Arctic tundra.

Even though MCD15A3 and MOD13A1 have not contributed to statistically significant results, there is potential for future applications, particularly for MCD15A3. This product generated a strong correlation ($R^2 = 0.8$, $p < 0.01$) and therefore, it may present as a useful LAI source once problems with overestimation are resolved.

5.2.2. Quality and availability of used materials

This section discusses several examples of possible sources of error associated with used materials. Satellite-derived data is practical in monitoring vegetation dynamics over large regions but in the recent years, studies have indicated uncertainty stemming from the lack of quality (Hilker et al., 2012). The MODIS vegetation products used in this study have been validated through a quality control assessment and, in some cases, corrected for atmospheric disturbances. Yet, noise and spectral inconsistencies are often imbedded in satellite-derived datasets and need to be accounted for.

PPFD, derived from PAR is one of the primary model inputs in this study. It has fine temporal resolution (3-hour) but it has the coarsest spatial resolution (5 km) of all the variables and therefore, it may not fully reflect the illumination conditions across the Arctic tundra. It was established (see section 3.6.) that PAR masked pixels were replaced by a static value, PAR = 0 W/m^2. This was done to 'unmask' the empty pixels and simulate neutral illumination conditions and to avoid possible NEE overestimation at the incident location. Furthermore, the inter-annual scope of this study is limited by the PAR availability (2008-2010). The Global Land Cover Facility (GLCF), accessible at www.landcover.org, is working towards an increased availability of PAR data and thus, there is a possibility of extending this study once an updated product is published. In addition, The European Space Agency (ESA) at www.sentinel.esa through collaboration with the Copernicus programme will introduce the Sentinel-satellite missions in the near future. Here, the PAR data could be accessed in ca. 1 km resolution, which would give a great incentive for further refinement of the PANEEx model.

Figure 8 depicts another example of error in this study. The screenshots of LAI raster images show the location surrounding the study site Kaamanen, Finland in 2009 and 2010. The right image (Fig. 8A) shows a discrepancy in LAI classification in form of unusually bright pixel values. The exact source of this error remains unknown; it is hypothesized that the error may be due to a satellite sensor inability to capture high reflection surfaces caused by, e.g. rain or standing water.

(A)

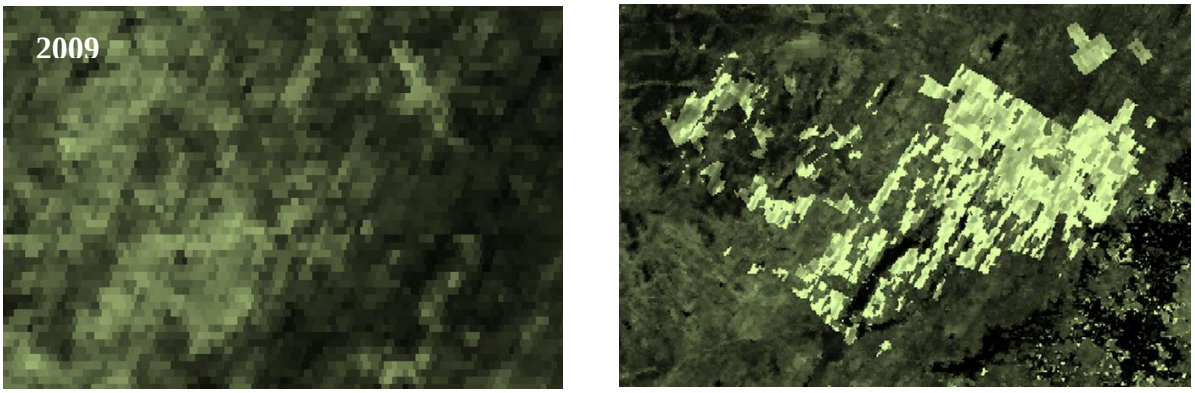

(B)

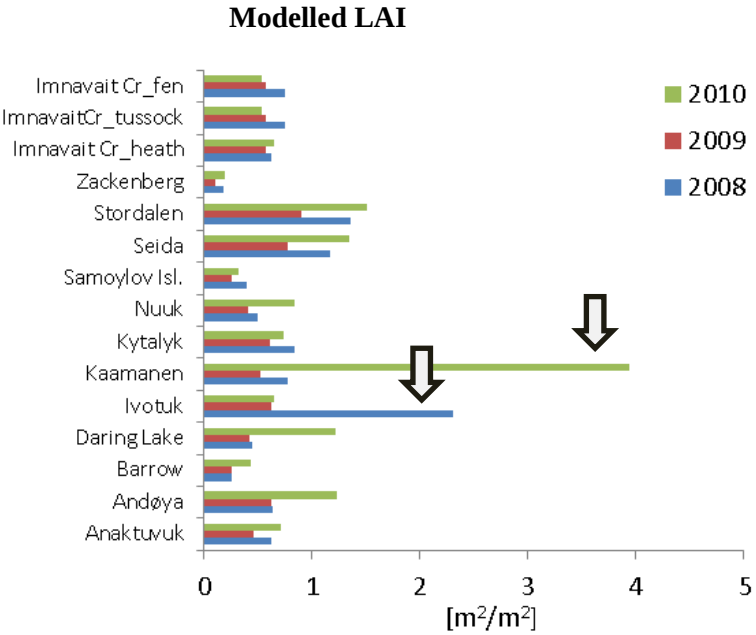

Figure 8. LAI spectral discrepancies. The two (A) images pertain to the same location at Kaamanen, Finland. The left image shows LAI for 2009 and the right one for 2010. The image in 2010 shows bright and geometrically confined LAI pixel values. This is also seen in a bar chart (B) that summarizes the retrieved LAI scores for all study sites during 2008 – 2010. The retrieved LAI scores are abnormally high in two cases, as shown by black arrows.

5.3.Future challenges

The results in this study have shown that implementation of PANEEx (Equation 2) model is useful in estimating NEE throughout the Arctic. A recent study by Mbufong et al., (In Prep) that employs the PANEEx model illustrates how integration of upscaling techniques with remotely sensed data can provide insight into spatial heterogeneity of Arctic NEE. Mbufong et al. (In Prep) produced a map (see Appendix 1) that characterizes average peak season NEE identifies regions of CO_2 uptake and release spanning from -4.5 to 0.5 μmol m^{-2} s^{-1}.

Knowledge gained from this thesis can reduce the uncertainty surrounding the representation of Arctic vegetation by MODIS vegetation products. There is a potential for improving the sensitivity of the PANEEx model by acquiring data in optimized spatial and temporal resolution. The European Space Agency (ESA) has been developing a new-generation Earth observation mission, the Sentinel satellites, consisting of a wide range of technologies in order to provide robust datasets of land, atmosphere and hydrosphere. In regards to future research in this matter, I recommend that inclusion of Sentinel 2 data as it would be a valuable contribution for global high-resolution monitoring of Earth (Martimort et al., 2007). In order to meet user's requirements, Sentinel 2 products Level-1B, Level-1C and Level-2A will be available in 10 m, 20 m and 60 m spatial resolution and capture of geophysical features, such as LAI, PAR, chlorophyll content, leaf water content, etc. (Verrelst J., 2013). In the future, these products could be considered as proxies in environmental modelling, leading to even more accurate NEE and LAI estimations.

6. Conclusions

The purpose of this study was to extend the current knowledge in environmental modelling and improve the understanding of relevance of vegetation satellite-derived data to modelling of Arctic NEE. The main objective in this thesis was to evaluate the suitability of four MODIS vegetation products in light of PANEEx NEE estimations in the circumpolar Arctic. The modelled NEE and LAI estimations were compared against 12 Arctic study sites. In doing so, it was demonstrated that individual MODIS products generate variations in modelled NEE and LAI, however, their accuracy differs depending on the configuration of each product. The conclusion drawn from study is that products MOD13Q1 followed by

MYDGA09 best simulate the NEE estimations compared to in situ observations. Here, the model estimated 78 % and 86 % of the measured fluxes with RMSE of 0.22 and 0.34 respectively.

In regards to the stated aims, the study has confirmed that the product with the finest resolution MOD13Q1 (250 m 16-day NDVI) generated the most accurate results. The results further show that this may not be always the case, given the second best estimation of NEE was modelled using MYD09GA (1 km daily NDVI). The findings in this thesis are supported by the reviewed literature. Other authors also employ 250 m vegetation indices in their research but it is imperative to mention that their methods differ.

Based on the comparisons with other studies, the following implications are identified for the future work on this matter: (1) the number of study sites (n = 12) may not be sufficient in a global study, (2) integration of multiple vegetation products through interpolation techniques may increase temporal resolution, thereby data availability and (3) attention should be paid to vegetation datasets with even finer spatial resolution than 250 m. Among the suggested improvements is, e.g. utilization of Sentinel 2 data (spatial resolution: 60 – 30 m), which has recently become available.

Acknowledgements

I would like to express my gratitude to all who have contributed to the production and revision of this thesis, especially to my supervisors: Dr. Andreas Persson and Dr. John Connolly for their patience and guidance through the thesis work. Also, I would like to acknowledge the rest of PANEEx Team, Dr. Herbert Mbufong and Dr. Magnus Lund for assistance with statistical analysis. Special thanks go to Dr. Lars Eklundh who indirectly contributed to this thesis by recommending me to the PANEEx project. This incentive gave me the opportunity to be involved in this large-scale scientific work. Personal thanks go to my relatives and friends who have supported me throughout the studies in Lund and never lost hope in me and David Kjellström for enormous help with java syntax design.

I am grateful to David Thau and the Google Earth Engine team for providing technical support during data processing and analysis and, most importantly, I am thankful for receiving funds for my research, which was facilitated through Google Earth Engine Research grant. I look forward to future collaborations.

Lastly, I would like to recognize the LP DAAC server for providing valuable data in this thesis. The and Information and images on MODIS products from 2008-2010 were obtained from https://lpdaac.usgs.gov/ maintained by the NASA EOSDIS Land Processes Distributed Active Archive Center (LP DAAC), USGS/Earth Resources Observation and Science (EROS) Center, Sioux Falls, South Dakota, 2016.

References

ACIA. 2005. Arctic Climate Impact Assessment. Scientific Report. Cambridge, UK:Cambridge University Press.

AMAP, 1998. AMAP Assessment Report: Arctic Pollution Issues. Arctic Monitoring and Assessment Programme (AMAP), Oslo, Norway. xii+859 pp. Anderson, K., 2015. Duality in climate science. *Nature Geoscience*. doi:10.1038/ngeo2559.

Anderson, K., 2015. Duality in climate science. Nature Geoscience. doi:10.1038/ngeo2559.

Angert, A., Biraud, S., Bonfils, C., Henning, C.C., Buerman, W., Pinzon, J., Tucker C.J., Fung, I., 2005. Drier summers cancel out the CO_2 uptake enhancement induced by warmer springs. Proc Natl Acad Sci USA. *Proceedings of the National Academy of Sciences of the United States of America* 102, 10823–7. doi:10.1073/pnas.0501647102.

Aurela, M., Laurila, T., Tuovinen, J.-P., 2004. The timing of snow melt controls the annual CO2 balance in a subarctic fen. *Geophys. Res. Lett*. 31, L16119. doi:10.1029/2004GL020315.

Baldocchi, D.D., 2003. Assessing the eddy covariance technique for evaluating carbon dioxide exchange rates of ecosystems: past, present and future. *Global Change Biology* 9, 479–492. doi:10.1046/j.1365-2486.2003.00629.x.

Boelman, N. T., Stieglitz, M., Rueth, H., Sommerkorn, M., Griffin, K. L., Shaver, G. R., Gamon, J. A., 2003. Response of NDVI, biomass, and ecosystem gas exchange to long-term warming and fertilization in wet sedge tundra. *Oecologia* 135:414–421.

Burba, G. G., McDermitt, D.K., Grelle, A., Anderson, D. J., Xu, L., 2008. Addressing the influence of instrument surface heat exchange on the measurements of CO_2 flux from open-path gas analyzers. *Global Change Biology* 14, 1854–1876. doi:10.1111/j.1365-2486.2008.01606.x.

Callaghan, T.V., Jonasson, C., Thierfelder, T., Yang, Z., Hedenås, H., Johansson, M., Molau, U., Van Bogaert, R., Michelsen, A., Olofsson, J., Gwynn-Jones, D., Bokhorst, S., Phoenix, G., Bjerke, J.W., Tømmervik, H., Christensen, T.R., Hanna, E., Koller, E.K., Sloan, V.L., 2013. Ecosystem change and stability over multiple decades in the Swedish subarctic: complex processes and multiple drivers. Philos. Trans. R. Soc. Lond., B, *Biol. Sci.* 368, 20120488. doi:10.1098/rstb.2012.0488.

Callaghan, T.V., Savela, H., DCE - Nationalt Center for Miljø og Energi, INTERACT (projekt), 2014. Interact: stories of Arctic science. Aarhus University, DCE - Danish Centre for Environment and Energy : INTERACT, [S.l.].

CAVM Team, (2003) Circumpolar Arctic Vegetation Map. (1:7,500,000 scale), Conservation of Arctic Flora and Fauna (CAFF) Map no. 1. U.S. Fish and Wildlife Service, Anchorage, AK, USA.

Chapman, W.L., Walsh, J.E., 1993. Recent Variations of Sea Ice and Air Temperature in High Latitudes. *Bull. Amer. Meteor. Soc*. 74, 33–47. doi:10.1175/1520-0477(1993)074<0033:RVOSIA>2.0.CO;2.

Christiansen, H.H., Etzelmüller, B., Isaksen, K., Juliussen, H., Farbrot, H., Humlum, O., Johansson, M., Ingeman-Nielsen, T., Kristensen, L., Hjort, J., Holmlund, P., Sannel,

A.B.K., Sigsgaard, C., Åkerman, H.J., Foged, N., Blikra, L.H., Pernosky, M.A., Ødegård, R.S., 2010. The thermal state of permafrost in the nordic area during the international polar year 2007–2009. *Permafrost Periglac. Process*. 21, 156–181. doi:10.1002/ppp.687.

Christensen, T.R., Jackowicz-Korczyński, M., Aurela, M., Crill, P., Heliasz, M., Mastepanov, M., Friborg, T., 2012. Monitoring the multi-year carbon balance of a subarctic palsa mire with micrometeorological techniques. *Ambio* 41 Suppl 3, 207–217. doi:10.1007/s13280-012-0302-5.

Comiso, J.C.and Parkinson, C.L., 2004. Satellite-observed changes in the Arctic. *Physics Today* 57, 38-44.

Faisal, K., AlAhmad, M., Shaker, A., 2012. Remote Sensing Techniques as a Tool for Environmental Monitoring. ISPRS - International Archives of the Photogrammetry, *Remote Sensing and Spatial Information Sciences* 39B8, 513–518. doi:10.5194/isprsarchives-XXXIX-B8-513-2012.

Fang, H., Jiang, C., Li, W., Wei, S., Baret, F., Chen, J.M., Garcia-Haro, J., Liang, S., Liu, R., Myneni, R.B., Pinty, B., Xiao, Z., Zhu, Z., 2013. Characterization and intercomparison of global moderate resolution leaf area index (LAI) products: Analysis of climatologies and theoretical uncertainties. *J. Geophys. Res. Biogeosci.* 118, 529–548. doi:10.1002/jgrg.20051.

Francis, J.A., 2013. The where and when of wetter and drier: disappearing Arctic sea ice plays a role. *Environ. Res. Lett*. 8, 041002. doi:10.1088/1748-9326/8/4/041002.

Frey, R. A., Ackerman, S. A., Liu, Y., Strabala, K. I., Zhang, H., Key, J. R., & Wang, X., 2008. Cloud detection with MODIS. Part I: Improvements in the MODIS cloud mask for collection 5. *Journal of Atmospheric and Oceanic Technology*, 25, 1057–1072.

Google Earth Engine Team, 2015. Google Earth Engine: A planetary-scale geospatial analysis platform. https://earthengine.google.com.

Hilker, T., Lyapustin, A.I., Tucker, C.J., Sellers, P.J., Hall, F.G., Wang, Y., 2012. Remote sensing of tropical ecosystems: Atmospheric correction and cloud masking matter. *Remote Sensing of Environment* 127, 370–384. doi:10.1016/j.rse.2012.08.035.

Didan, K. and Huete, A., 2006. Collection 5 Change Summary. MODIS Vegetation Index Product Series. TBRS Lab., The University of Arizona, 1-17 pp.

INTERACT, 2015. INTERACT Stories of Arctic Science. Eds.: Callaghan, T.V. and Savela, H. DCE – Danish Centre for Environment and Energy, Aarhus University, Denmark, 180 pp.

IPCC, 2014: Summary for policymakers. In: Climate Change 2014: Impacts,Adaptation, and Vulnerability. Part A: Global and Sectoral Aspects. Contribution of Working Group II to the Fifth Assessment Report of the Intergovernmental Panel on Climate Change [Field, C.B., V.R. Barros, D.J. Dokken, K.J. Mach, M.D. Mastrandrea, T.E. Bilir, M. Chatterjee, K.L. Ebi, Y.O. Estrada, R.C. Genova, B. Girma, E.S. Kissel, A.N. Levy, S. MacCracken, P.R. Mastrandrea, and L.L.White (eds.)]. Cambridge University Press, Cambridge, United Kingdom and New York, NY, USA, pp. 1-32.a

Jensen, L. M. and Rasch, M. (Eds.), 2008. Nuuk Ecological Research Operations, 1st Annual Report, 2007. – Copenhagen, Danish Polar Centre, Danish Agency for Science, Technology and Innovation, Ministry of Science, Technology and Innovation, 2008.

Johansson, M., Åkerman, J., Jonasson, C., Christensen, T., Callaghan, T.V., 2008. Increasing Permafrost Temperatures in Subarctic Sweden, in: [Publication Information Missing]. Presented at the Ninth international conference on Permafrost, pp. 851–856.

Kalnay, E., Kanamitsu, M., Kistler, R., Collins, W., Deaven, D., Gandin, L., Iredell, M., Saha, S., White, G., Woollen, J., Zhu, Y., Leetmaa, A., Reynolds, R., Chelliah, M., Ebisuzaki, W., Higgins, W., Janowiak, J., Mo, K.C., Ropelewski, C., Wang, J., Jenne, R., Joseph, D., 1996. The NCEP/NCAR 40-Year Reanalysis Project. *Bull. Amer. Meteor. Soc.* 77, 437–471. doi:10.1175/1520-0477(1996)077<0437:TNYRP>2.0.CO;2.

Kimball, J., Jones, L., Zhang, K., Heinsch, F., McDonald, K., Oechel, W., 2009. A Satellite Approach to Estimate Land-Atmosphere CO_2 Exchange for Boreal and Arctic Biomes Using MODIS and AMSR-E. *IEEE Transactions on Geoscience and Remote Sensing* 47, 569–587.

Kutzbach, L., Wille, C., Pfeiffer, E.-M., 2007. The exchange of carbon dioxide between wet arctic tundra and the atmosphere at the Lena River Delta, Northern Siberia. *Biogeosciences* 4, 869–890. doi:10.5194/bg-4-869-2007.

Kwon, H.-J., Oechel, W.C., Zulueta, R.C., Hastings, S.J., 2006. Effects of climate variability on carbon sequestration among adjacent wet sedge tundra and moist tussock tundra ecosystems. *J. Geophys*. Res. 111, G03014. doi:10.1029/2005JG000036.

Lafleur, P.M., Humphreys, E.R., 2008. Spring warming and carbon dioxide exchange over low Arctic tundra in central Canada. *Global Change Biology* 14, 740–756. doi:10.1111/j.1365-2486.2007.01529.x.

Land Processes Distributed Active Archive Center (LP DAAC), 2000, Land Surface Temperature and Emissivity Daily L3 Global 1 km Grid SIN. Version 005. NASA EOSDIS Land Processes DAAC, USGS Earth Resources Observation and Science (EROS) Center, Sioux Falls, South Dakota (https://lpdaac.usgs.gov), accessed 01/20, 2015, at https://lpdaac.usgs.gov/dataset_discovery/modis/modis_products_table/mod11a1.

Land Processes Distributed Active Archive Center (LP DAAC), 2000. Land Cover Type Yearly L3 Global 500 m SIN Grid. Version 051. NASA EOSDIS Land Processes DAAC, USGS Earth Resources Observation and Science (EROS) Center, Sioux Falls, South Dakota (https://lpdaac.usgs.gov), accessed 04/11, 2015, at https://lpdaac.usgs.gov/dataset_discovery/modis/modis_products_table/mcd12q1.

Land Processes Distributed Active Archive Center (LP DAAC), 2002, Leaf Area Index – Fraction of Photosynthetically Active Radiation 4-Day L4 Global 1km. Version 005. NASA EOSDIS Land Processes DAAC, USGS Earth Resources Observation and Science (EROS) Center, Sioux Falls, South Dakota (https://lpdaac.usgs.gov), accessed 02/26, 2016, at https://lpdaac.usgs.gov/dataset_discovery/modis/modis_products_table/mcd15a3

Lattin, J.M., Carroll, J.D., Green, P.E., Green, P.E., 2003. Analyzing multivariate data. Thomson Brooks/Cole, Pacific Grove, CA.

Li, Z., Tang, H., Xin, X., Zhang, B., Wang, D., 2014. Assessment of the MODIS LAI Product Using Ground Measurement Data and HJ-1A/1B Imagery in the Meadow Steppe of Hulunber, China. *Remote Sensing* 6, 6242–6265. doi:10.3390/rs6076242.

Liang, S., Zhao, X., Liu, S., Yuan, W., Cheng, X., Xiao, Z., Zhang, X., Liu, Q., Cheng, J., Tang, H., Qu, Y., Bo, Y., Qu, Y., Ren, H., Yu, K., Townshend, J., 2013. A long-term Global LAnd Surface Satellite (GLASS) data-set for environmental studies. *International Journal of Digital Earth* 6, 5–33. doi:10.1080/17538947.2013.805262.

Longley, P. (Ed.), 2005. Geographical information systems and science, 2nd ed. ed. Wiley, Chichester ; Hoboken, NJ.

Lund, M., Bjerke, J.W., Drake, B.G., Engelsen, O., Hansen, G.H., Parmentier, F.J.W., Powell, T.L., Silvennoinen, H., Sottocornola, M., Tømmervik, H., Weldon, S., Rasse, D.P., 2015. Low impact of dry conditions on the CO 2 exchange of a Northern-Norwegian blanket bog. *Environmental Research Letters* 10, 25004. doi:10.1088/1748-9326/10/2/025004.

Lund, M., Falk, J. M., Friborg, T., Mbufong, H. N., Sigsgaard, C., Soegaard, h., Tamstorf, M.P. 2012. Trends in CO_2 exchange in a high Arctic tundra heath, 2000-2010, J. *Geophys. Res*., pp 117, G02001, doi10.1029/2011JG001901.

Luus, K.A., Lin, J.C., Kelly, R.E.J., Duguay, C.R., 2013. Subnivean Arctic and sub-Arctic net ecosystem exchange (NEE) Towards representing snow season processes in models of NEE using cryospheric remote sensing. *Progress in Physical Geography* 37, 484–515. doi:10.1177/0309133313491130.

Martimort, P., Arino, O., Berger, M., Biasutti, R., Carnicero, B., Bello, U.D., Fernandez, V., Gascon, F., Greco, B., Silvestrin, P., Spoto, F., Sy, O., 2007. Sentinel-2 optical high resolution mission for GMES operational services, in: 2007 *IEEE International Geoscience and Remote Sensing Symposium*. Presented at the 2007 IEEE International Geoscience and Remote Sensing Symposium, pp. 2677–2680. doi:10.1109/IGARSS.2007.4423394.

Marushchak, M.E., Kiepe, I., Biasi, C., Elsakov, V., Friborg, T., Johansson, T., Soegaard, H., Virtanen, T., Martikainen, P.J., 2013. Carbon dioxide balance of subarctic tundra from plot to regional scales. *Biogeosciences* 10, 437–452. doi:10.5194/bg-10-437-2013.

Matveyeva, N.V., 1998. Zonation of Plant Cover in the Arctic. Russian Academy of Science. St. Petersburg. 21. 220.

Mbufong, H. N., 2015. Drivers of seasonality in Arctic carbon dioxide fluxes. PhD thesis. Arhus University, Department of Bioscience, Denmark. 144 pp.

Mbufong, H.N., Kusbach, A., Lund, M., Christensen T.R., Persson, A., Tamstorf, M.P., Connolly, J., (In Prep). Measurement-based upscaling of pan Arctic net ecosystem exchange: the PANEEx project.

Mbufong, H.N., Lund, M., Aurela, M., Christensen, T.R., Eugster, W., Friborg, T., Hansen, B.U., Humphreys, E.R., Jackowicz-Korczynski, M., Kutzbach, L., Lafleur, P.M., Oechel, W.C., Parmentier, F.J.W., Rasse, D.P., Rocha, A.V., Sachs, T., van der Molen, M.K., Tamstorf, M.P., 2014. Assessing the spatial variability in peak season CO_2 exchange characteristics across the Arctic tundra using a light response curve parameterization. Biogeosciences 11, 4897-4912.

McGuire, A.D., III, F.S.C., Walsh, J.E., Wirth, C., 2006. Integrated Regional Changes in Arctic Climate Feedbacks: Implications for the Global Climate System. *Annual Review of Environment and Resources* 31, 61–91. doi:10.1146/annurev.energy.31.020105.100253.

McGuire, A.D., Hayes, D.J., Kicklighter, D.W., Manizza, M., Zhuang, Q., Chen, M., Follows, M.J., Gurney, K.R., McClelland, J.W., Melillo, J.M., Peterson, B.J., Prinn, R.G., 2010. An analysis of the carbon balance of the Arctic Basin from 1997 to 2006. Tellus B 62. doi:10.3402/tellusb.v62i5.16587.

McMichael, C.E., 1999. Estimating CO_2 exchange at two sites in Arctic tundra ecosystems during the growing season using a spectral vegetation index. *International Journal of Remote Sensing* 20, 683–698. doi:10.1080/014311699213136.

Meijering, E., 2002. A chronology of interpolation: from ancient astronomy to modern signal and image processing. *Proceedings of the IEEE* 90, 319–342. doi:10.1109/5.993400.

Myneni, R.B., Ramakrishna, R., Nemani, R., Running, S.W., 1997. Estimation of global leaf area index and absorbed par using radiative transfer models. *IEEE Transactions on Geoscience and Remote Sensing* 35, 1380–1393. doi:10.1109/36.649788.

Oechel, W.C. and Vourlitis, G.L., 1996. Direct Effects of Elevated CO_2 on Arctic Plant and Ecosystem Function, in: Carbon Dioxide and Terrestrial Ecosystems. *Elsevier*, pp. 163–176.

Overland, J., Francis, J.A., Hall, R., Hanna, E., Kim, S.-J., Vihma, T., 2015. The Melting Arctic and Midlatitude Weather Patterns: Are They Connected? *J. Climate* 28, 7917–7932. doi:10.1175/JCLI-D-14-00822.1.

Parmentier, F.J.W., van der Molen, M.K., van Huissteden, J., Karsanaev, S.A., Kononov, A.V., Suzdalov, D.A., Maximov, T.C., Dolman, A.J., 2011. Longer growing seasons do not increase net carbon uptake in the northeastern Siberian tundra. J. *Geophys. Res*. 116, G04013. doi:10.1029/2011JG001653.

Piao, S., Ciais, P., Friedlingstein, P., Peylin, P., Reichstein, M., Luyssaert, S., Margolis, H., Fang, J., Barr, A., Chen, A., Grelle, A., Hollinger, D.Y., Laurila, T., Lindroth, A., Richardson, A.D., Vesala, T., 2008. Net carbon dioxide losses of northern ecosystems in response to autumn warming. *Nature* 451, 49–52. doi:10.1038/nature06444.

Rocha, A.V. and Shaver, G.R., 2011. Burn severity influences postfire CO_2 exchange in arctic tundra. *Ecol Appl* 21, 477–489.

Schubert, P., Lagergren, F., Aurela, M., Christensen, T., Grelle, A., Heliasz, M., Klemedtsson, L., Lindroth, A., Pilegaard, K., Vesala, T., Eklundh, L., 2012. Modeling GPP in the Nordic forest landscape with MODIS time series data—Comparison with the MODIS GPP product. *Remote Sensing of Environment* 126, 136–147. doi:10.1016/j.rse.2012.08.005.

Screen, J. A. and Simmonds, I., 2010. The central role of diminishing sea ice in recent Arctic temperature amplification, *Nature*, 464, 13341337, doi:10.1038/nature09051.

Serreze, M.C., Barrett, A.P., Stroeve, J.C., Kindig, D.N., Holland, M.M., 2009. The emergence of surface-based Arctic amplification. *The Cryosphere* 3, 11–19. doi:10.5194/tc-3-11-2009.

Liang, S. and Zhang, X., 2012. Global Land Surface Products: Photosynthetically Active Radiation Data Collection (2008-2010), Beijing Normal University. doi:10.6050/glass863.3005.db.

Stiegler, C., 2016. Surface energy exchange and land-atmosphere interactions of Arctic and subarctic tundra ecosystems under climate change. PhD Thesis. Lund, Sweden: Lund University.

Stocker, T.F., D. Qin, G.-K. Plattner, L.V. Alexander, S.K. Allen, N.L. Bindoff, F.-M. Bréon, J.A. Church, U. Cubasch, S. Emori, P. Forster, P. Friedlingstein, N. Gillett, J.M. Gregory, D.L. Hartmann, E. Jansen, B. Kirtman, R. Knutti, K. Krishna Kumar, P. Lemke, J. Marotzke, V. Masson-Delmotte, G.A. Meehl, I.I. Mokhov, S. Piao, V. Ramaswamy, D. Randall, M. Rhein, M. Rojas, C. Sabine, D. Shindell, L.D. Talley, D.G. Vaughan and S.-P. Xie, 2013. Technical Summary. In: Climate Change 2013: The Physical Science Basis. *Contribution of Working Group I to the Fifth Assessment Report of the Intergovernmental Panel on Climate Change* [Stocker, T.F., D. Qin, G.-K. Plattner, M. Tignor, S.K. Allen, J. Boschung, A. Nauels, Y. Xia, V. Bex and P.M. Midgley (eds.)]. Cambridge University Press, Cambridge, United Kingdom and New York, NY, USA.

Stow, D., Hope, A., Boynton, W., Phinn, S., Walker, D., Auerbach, N., 1998. Satellite-derived vegetation index and cover type maps for estimating carbon dioxide flux for arctic tundra regions. *Geomorphology, Application of remote sensing and GIS in geomorphology* 21, 313–327. doi:10.1016/S0169-555X(97)00071-8.

Stoy, P.C., Williams, M., Evans, J.G., Prieto-Blanco, A., Disney, M., Hill, T.C., Ward, H.C., Wade, T.J., Street, L.E., 2013. Upscaling Tundra CO_2 Exchange from Chamber to Eddy Covariance Tower. Arctic, *Antarctic, and Alpine Research* 45, 275–284. doi:10.1657/1938-4246-45.2.275.

Street, L.E., Stoy, P.C., Sommerkorn, M., Fletcher, B.J., Sloan, V.L., Hill, T.C., Williams, M., 2012. Seasonal bryophyte productivity in the sub-Arctic: a comparison with vascular plants. *Functional Ecology* 26, 365–378. doi:10.1111/j.1365-2435.2011.01954.x.

Tang, J., Miller, P.A., Persson, A., Olefeldt, D., Pilesjö, P., Heliasz, M., Jackowicz-Korczynski, M., Yang, Z., Smith, B., Callaghan, T.V., Christensen, T.R., 2015. Carbon budget estimation of a subarctic catchment using a dynamic ecosystem model at high spatial resolution. *Biogeosciences* 12, 2791–2808. doi:10.5194/bg-12-2791-2015.

Tang, X., Wang, Z., Liu, D., Song, K., Jia, M., Dong, Z., Munger, J.W., Hollinger, D.Y., Bolstad, P.V., Goldstein, A.H., Desai, A.R., Dragoni, D., Liu, X., 2012. Estimating the net ecosystem exchange for the major forests in the northern United States by integrating MODIS and AmeriFlux data. *Agricultural and Forest Meteorology* 156, 75–84. doi:10.1016/j.agrformet.2012.01.003.

Tape, K.D., Hallinger, M., Welker, J.M., Ruess, R.W., 2012. Landscape Heterogeneity of Shrub Expansion in Arctic Alaska. Ecosystems 15, 711–724. doi:10.1007/s10021-012-9540-4.

Van Wijk, M. T. and Williams, M., 2005. Optical Instruments for Measuring Leaf Area Index in Low Vegetation: Application in Arctic Ecosystems. Ecological Applications, 15: 1462–1470. doi:10.1890/03-5354y.

Van Wijk, M. T., Williams, M. and Shaver, G. R., 2005. Tight coupling between leaf area index and foliage N content in arctic plant communities. *Oecologia* 142: 421–427.

Vermote, E. F., Kotchenova, S. Y., and Ray, J. P., 2008. MODIS surface reflectance user's guide v 1.2.at http://modis-sr.ltdri.org.

Verrelst, J., Rivera, J.P., Moreno, J., Camps-Valls, G., 2013. Gaussian processes uncertainty estimates in experimental Sentinel-2 LAI and leaf chlorophyll content retrieval. *ISPRS Journal of Photogrammetry and Remote Sensing* 86, 157–167. doi:10.1016/j.isprsjprs.2013.09.012.

Watts, J.D., Kimball, J.S., Jones, L.A., Schroeder, R., McDonald, K.C., 2012. Satellite Microwave remote sensing of contrasting surface water inundation changes within the Arctic–Boreal Region. *Remote Sensing of Environment* 127, 223–236. doi:10.1016/j.rse.2012.09.003.

Watts, J.D., Kimball, J.S., Parmentier, F.J.W., Sachs, T., Rinne, J., Zona, D., Oechel, W., Tagesson, T., Jackowicz-Korczyński, M., Aurela, M., 2014. A satellite data driven biophysical modeling approach for estimating northern peatland and tundra CO_2 and CH4 fluxes. *Biogeosciences* 11, 1961–1980. doi:10.5194/bg-11-1961-2014.

Westergaard-Nielsen, A., Lund, M., Hansen, B.U., Tamstorf, M.P., 2013. Camera derived vegetation greenness index as proxy for gross primary production in a low Arctic wetland area. *ISPRS Journal of Photogrammetry and Remote Sensing* 86, 89–99. doi:10.1016/j.isprsjprs.2013.09.006.

Williams, M., Rastetter, E.B., Shaver, G.R., Hobbie, J.E., Carpino, E., Kwiatkowski, B.L., 2001. Primary Production of an Arctic Watershed: An Uncertainty Analysis. *Ecological Applications* 11, 1800–1816. doi:10.1890/1051-0761(2001)011[1800:PPOAAW]2.0.CO;2.

Williams, M., Street, L.E., Wijk, M.T. van, Shaver, G.R., 2006. Identifying Differences in Carbon Exchange among Arctic Ecosystem Types. Ecosystems 9, 288–304. doi:10.1007/s10021-005-0146-y.

Xiao, Z., Liang, S., Wang, J., Chen, P., Yin, X., 2013a. "Leaf Area Index Retrieval from Multi-Sensor Remote Sensing Data Using General Regression Neural Networks." IEEE *Transactions on Geoscience and Remote Sensing*.

Xiao, Z., Liang, S., Wang, J., Zhao, X., 2013b. "Long Time Series Global Land Surface Satellite (GLASS) Leaf Area Index Product Derived from MODIS and AVHRR Data." *Remote Sensing of Environment*, submitted.

Zhao, X., Liang, S., Liu, S., Yuan, W., Xiao, Z., Liu, Q., Cheng, J., Zhang, X., Tang, H., Zhang, X., Liu, Q., Zhou, G., Xu, S., Yu, K., 2013. The Global Land Surface Satellite (GLASS) Remote Sensing Data Processing System and Products. *Remote Sensing 5*, 2436–2450. doi:10.3390/rs5052436.

Åkerman, H.J., 1982. Observations of palsas within the continuous permafrost zone in eastern Siberia and in Svalbard. *Geografisk Tidsskrift-Danish Journal of Geography* 82, 45–51. doi:10.1080/00167223.1982.10649150.

Åkerman, H.J., Johansson, M., 2008. Thawing permafrost and thicker active layers in sub-arctic Sweden. *Permafrost Periglac. Process*. 19, 279–292. doi:10.1002/ppp.626.

Appendix

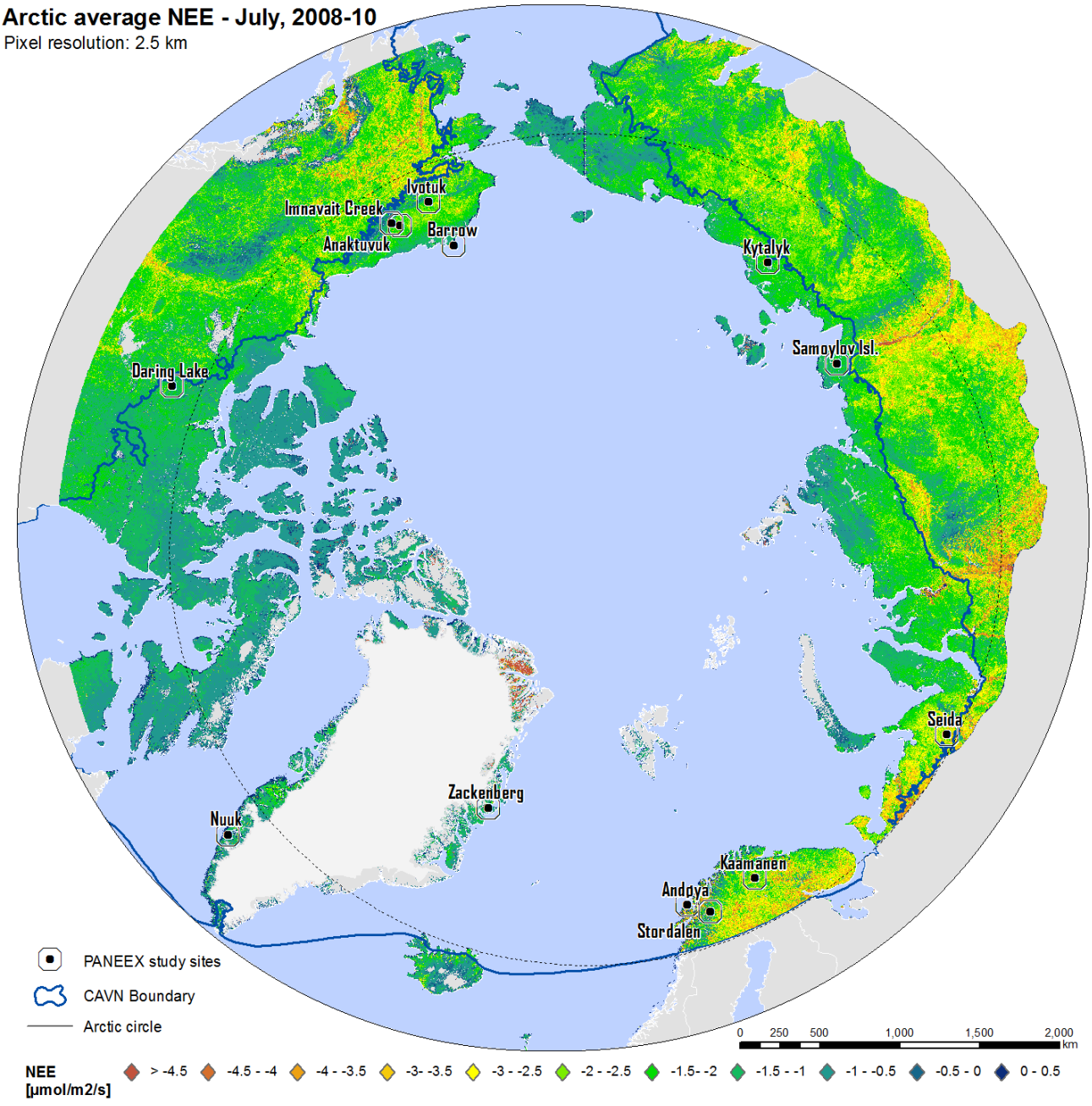

Appendix 1. Global mean July Arctic NEE 2008-2010. Map illustrates spatial heterogeneity of NEE throughout Arctic tundra. Source: Mbufong et al., (In Prep).

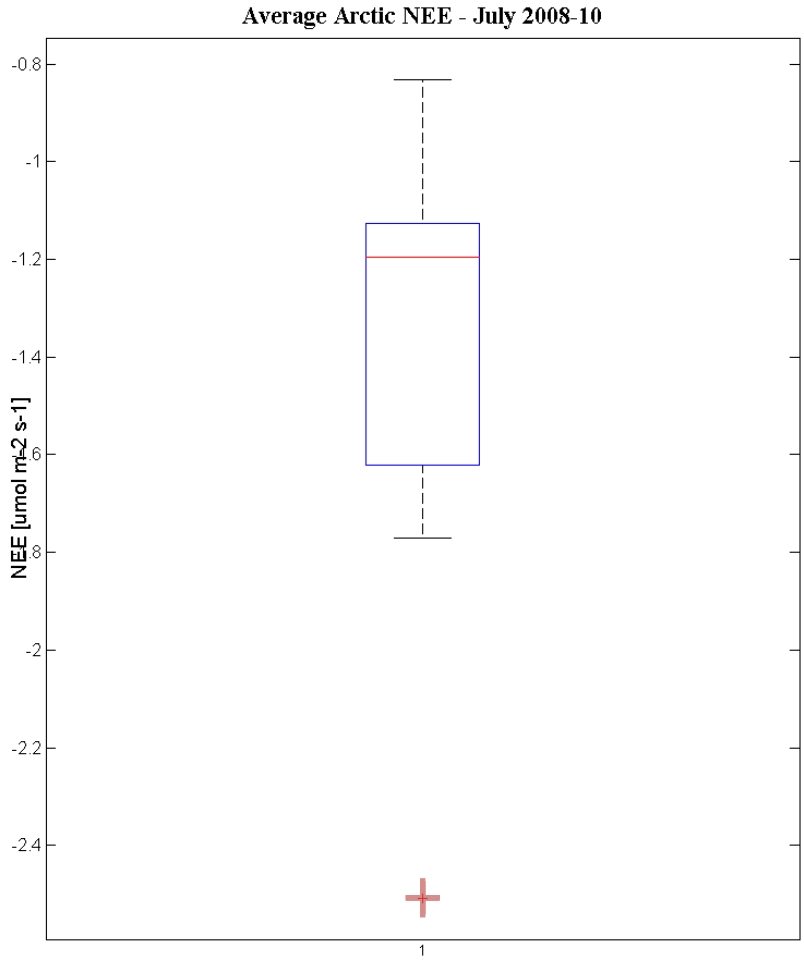

Appendix 2. The boxplot analysis shows average Arctic NEE 2008-10 based on MOD13A1 LAI. An outlier has been identified and is displayed as red cross.